

OFF-LOADING-LINE MOTION COMPENSATION  
ON VESSELS

---

A Thesis  
Presented to  
the Faculty of the Graduate School  
University of Houston

---

In Partial Fulfillment  
of the Requirements for the Degree  
Master of Science in Mechanical Engineering

---

by  
Mohamad Fakharmanesh

December 1975

## ACKNOWLEDGEMENT

The author wishes to express his appreciation to Dr. Ray Nachlinger and Professor William Schneider for their help and guidance during the thesis research and preparation.

— — — —

OFF-LOADING-LINE MOTION COMPENSATION  
ON VESSELS

---

An Abstract  
Presented to  
the Faculty of the Graduate School  
University of Houston

---

In Partial Fulfillment  
of the Requirements for the Degree  
Master of Science in Mechanical Engineering

---

by  
Mohamad Fakharmanesh  
December 1975

## ABSTRACT

Here, several problems due to vessel motions during load handling on a floating vessel and their consequences are presented. In particular, off loading using a cable and winch is considered in detail. The cable is simplified as a spring with its mass attached to its end. The effect of this cable on payload motion is investigated and the need for controlling the payload motion for safe operation is clearly indicated. It is shown that a control system using feedback signals from the lower end of the cable can effectively eliminate undesired motions of the payload even during reasonably large vessel motions. A typical system is designed which will provide satisfactory performance and which requires only a nominal amount of winch power. The major, but solvable, problem is the transmission of the feedback signals from the end of the cable.

## TABLE OF CONTENTS

	Page
LIST OF FIGURES . . . . .	III
LIST OF TABLES . . . . .	V
Chapter	
I. INTRODUCTION . . . . .	1
II. MOTION OF MASSES LOCATED AT THE END OF A CABLE . . . . .	9
1. Equations . . . . .	9
2. Calculations . . . . .	15
III. WINCH AND CABLE TRANSFER FUNCTIONS . .	20
1. Equations . . . . .	20
2. Block Diagrams . . . . .	22
IV. OPEN LOOP SYSTEM PERFORMANCE (D-C ARMATURE CONTROL MOTOR DRIVING UNIT) . . . . .	25
V. CLOSED LOOP SYSTEM PERFORMANCE . . . .	32
VI. WINCH CONTROL SYSTEM MOTION REQUIREMENTS . . . . .	37
VII. SHIP RESPONSE IN HEAVE . . . . .	40
VIII. CALCULATIONS FOR CHOOSING THE COMPONENTS OF THE WINCH SYSTEM AND THE CONTROL SYSTEM . . . . .	45
1. Winch System . . . . .	45
2. Control System . . . . .	48
IX. CONCLUSIONS . . . . .	60
BIBLIOGRAPHY . . . . .	62

## APPENDIXES

A.	THE CALCULATION OF THE APPARENT OR VIRTUAL MASS . . . . .	64
B.	DETERMINATION OF THE WAVES SPECTRUM FROM SIGNIFICANT WAVE HEIGHTS AND WAVE PERIODS . . . . .	67

### III

#### LIST OF FIGURES

Figure	Page
1. Oscillation Modes of a Floating Vessel	2
2. Wave-Height Data for the North Atlantic	4
3. Vessel and Cable Model	10
4. Vessel and Cable Block Diagram	10
5. Cable Model	11
6-11. Frequency Response of the Cable (Bode Plot)	17-19
12,13. Winch and Cable Block Diagram	23,24
14. D-C Armature Control Motor	25
15-17. Open Loop Block Diagram of the System	28-30
18. Closed Loop Block Diagram of the System	33
19. Relationship Between Ship Motion and Payload Motion	34
20. Closed Loop Block Diagram of the System	38
21. Relationship Between Ship Motion and Drum Motion	39
22. Heave Response	41
23. Frequency Spectrum	41
24. Heave Amplification Operator	42
25. Ship Response in Heave	42
26. GE-752 Motor Curves	47
27. Frequency Response of Payload Motion with Respect to Ship Motion (Bode Plot)	50

#### IV

Figure	Page
28. Frequency Response of Drum Motion with Respect to Ship Motion (Bode Plot)	50
29. Frequency Spectrum for Payload Due to Heave Motion Before Compensation	52
30. Frequency Spectrum for Payload Due to Heave Motion After Compensation	54
31. Compensated Payload Motion Due to a Unit Sinusoidal Ship Motion for the Frequencies Shown	56
32. Sensitivity Test	57
33. Payload Motion Due to a Unit Step Voltage Change at Winch Control	58
B-1. Non-dimensional Period Spectrum	68
B-2. Non-dimensional Frequency Spectrum	68



## LIST OF TABLES

Table	Page
1. Oscillation Modes of a Vessel	2
2. Wave Height for Safe, Efficient Operation for Some Ships	3
3. Wind and Sea Scale for Fully Arisen Sea	6
4. Drag Coefficient Data for Selected Objects	14
5. Ship Response in Heave	43
6. Model 1000 American Hoist Specifications	46
7. Frequency Response of Payload Motion and Drum Motion with Respect to Ship Motion	51
8. Frequency Spectrum for Payload Due to Heave Motion Before Compensation	53
9. Frequency Spectrum for Payload Due to Heave Motion After Compensation	55
A-1. Hydrodynamic Mass Factor	65
B-1. Non-dimensional Period Spectrum	69
B-2. Non-dimensional Frequency Spectrum	70

## CHAPTER I

## INTRODUCTION

The problem of ship motions (indicated in Figure 1 and Table 1) [1],\* became a topic of special interest in offshore technology when the oil industry started drilling in deep water from floating vessels.

Heave, pitch and roll motions (specially those with the high amplitudes) produce problems in performing the following load handling tasks:

1. Loading or unloading from one floating vessel to another floating vessel.
2. Loading or unloading from a floating vessel to a fixed platform or vice versa.
3. Raising or lowering massive structures in the water.
4. Supporting structures for a "fixed" position in the water for assembling purposes.

Table 2 [2] indicates the wave height for safe and efficient work operations for some ships. In the case of semisubmersibles, the "safe" wave height is greater, but not tremendously so, from Figure 2 [3] as a typical example

\*Numbers in brackets designate references in the Bibliography on page 62.

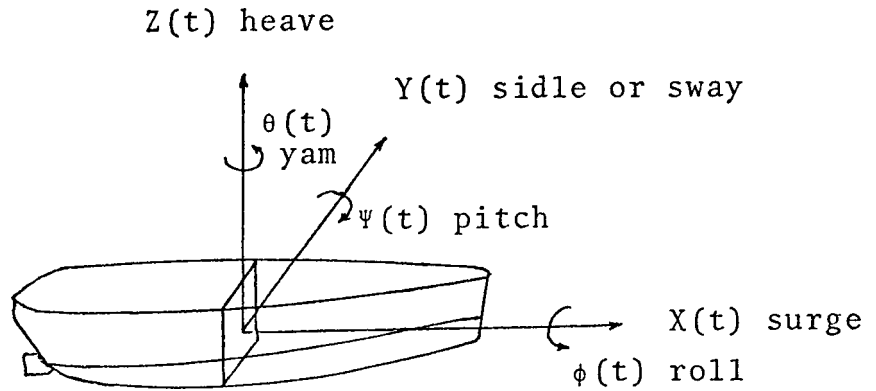


Figure 1. Oscillation Modes of a Floating Vessel

TABLE 1

OSCILLATION MODES OF A VESSEL

Axis	Translatory Oscillation		Rotary Oscillation	
	Type	Symbol	Type	Symbol
Longitudinal	Surge	X	Roll	$\phi$
Transverse	Sway	Y	Pitch	$\psi$
Vertical	Heave	Z	Yam	$\theta$

TABLE 2

WAVE HEIGHT FOR SAFE, EFFICIENT  
OPERATION FOR SOME SHIPS

Type of Operation	Wave Heights (Meter) For*		
	Safe, Efficient Operation	Marginal Operation	Dangerous and/or Inefficient Operation
Crew boats, 20-30 meters in length Loading or unloading crews at platform	0-.9	.9-1.5	>1.5
Supervisor's boats, fast craft 10-16 meters in length Loading or unloading personnel at plat- form or floating equipment	0-.6	.6-1.2	>1.2
LCT-type vessel and cargo luggers Loading or unloading at platform Loading or unloading at floating equipment	0-.9	.9-1.2	>1.2
	0-1.2	1.2-1.5	>1.5
Buoy laying (using small derrick barge)	0-.6	.6-.9	>.9
Platform building Using ship-mounted derrick Using large derrick barge	0-1.2	1.2-1.8	>1.8
	0-.9	.9-1.5	>1.5

\*Wave heights used are those of the average maximum waves. Height limits given are not rigid and will vary to some extent with locality, local wind conditions, experience of personnel, etc.

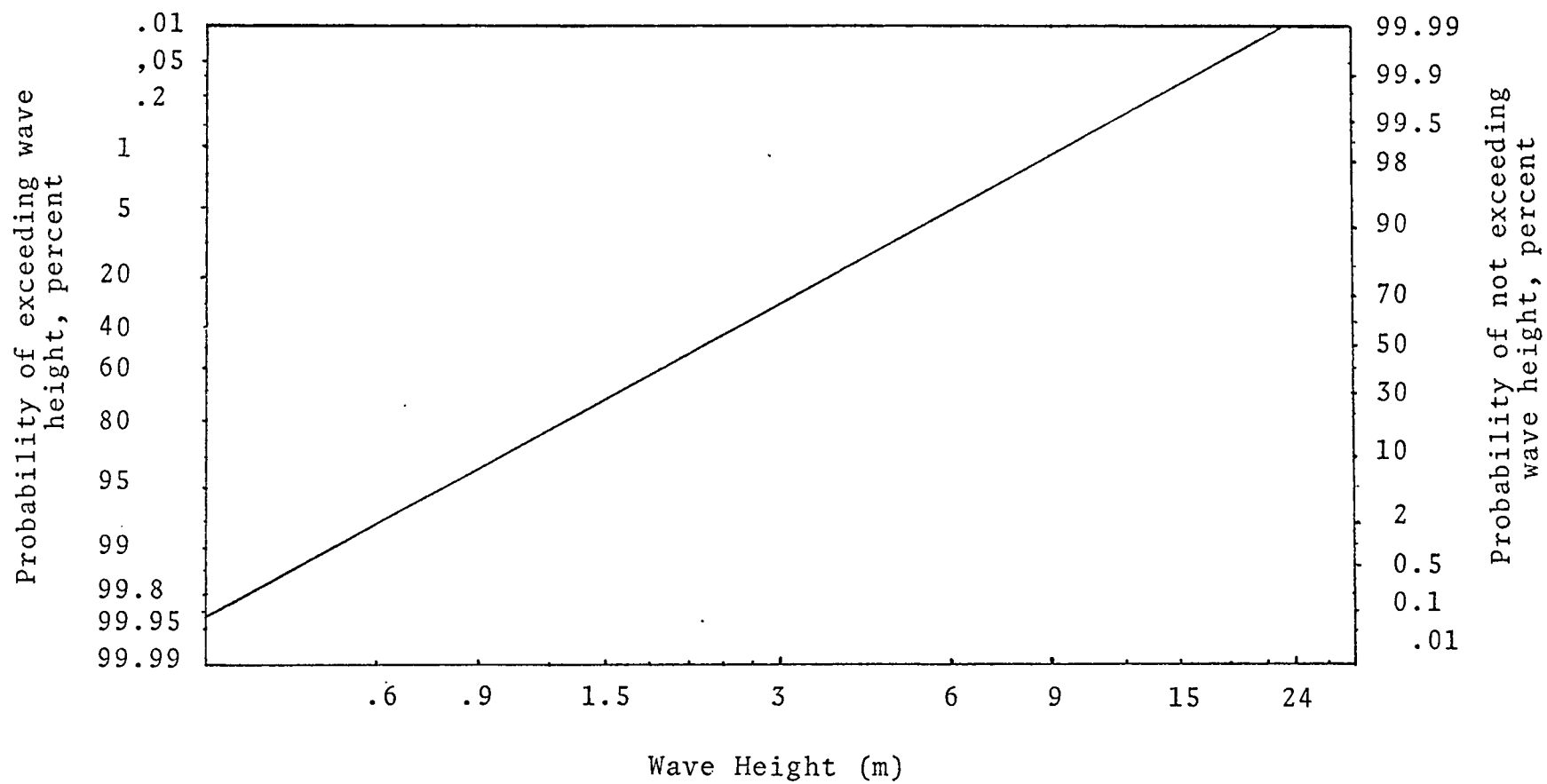


Figure 2. Wave-Height Data for the North Atlantic

in the North Atlantic, it is clear that the probability of wave heights exceeding the safe height is high; sea state 5 (Table 3) [4] can be considered as a typical sea state in most cases.

From the above discussion, it can be concluded that either the operations should be performed when the wave heights are in the safe range, or the handling equipment should compensate for the ship motion. Available motion compensators have been helpful in allowing an increase in the wave heights during which safe operations can be done, but because of design deficiencies inherent in the system and other restrictions, they are not completely successful. Consequently, even with the use of actual motion compensators, it is still generally necessary to wait for a good sea state condition; obviously, this is not economical.

One of the more successful motion compensators is the "constant tension" winch [5]. In this winch, constant cable tension is maintained by a closed-loop servo system that utilizes upper end cable tension as the primary feedback. As the vessel rises or falls, the tension increases or decreases respectively. An increase in cable tension will cause the winch to "pay out" cable, while a decrease in tension will cause the winch to "haul in" cable. The term "constant tension" is really a misnomer, since the system requires a finite signal (tension change), even though it is very small, to operate the winch unit.

TABLE 3

## WIND AND SEA SCALE FOR FULLY ARISEN SEA

Sea State	Description	Wind Velocity Knots	Sea			
			Wave Height, feet		Significant Range of Periods, sec	Average Period
			Average	Significant		
0	Sea like a mirror.	0	0	0		
	Ripples with the appearance of scales are formed, but without foam crests.	2	.05	.08	Up to 1.2 sec	.5
1	Small wavelets, still short but more pronounced.	5	.18	.29	.4-2.8	1.4
	Large wavelets, crests begin to break	8.5	.6	1.0	.8-5.0	2.4
2		10	.88	1.4	1.0-6.0	2.9
3	Small waves, becoming larger, fairly frequent white horses.	12	1.4	2.2	1.0-7.0	3.4
		13.5	1.8	2.9	1.4-7.6	3.9
		14	2.0	3.3	1.5-7.8	4.0
		16	2.9	4.6	2.0-8.8	4.6

TABLE 3 (Continued)

Sea State	Description	Wind Velocity Knots	Sea			
			Wave Height, feet		Significant Range Periods, sec	Average Period
			Average	Significant		
4	Moderate waves, taking a more pronounced form; white horses are formed.	18	3.8	6.1	2.5-10.0	5.1
		19	4.3	6.9	2.8-10.6	5.4
		20	5.0	8.0	3.0-11.1	5.7
5	Large waves begin to form; the white foam crests are more	22	6.4	10	3.4-12.2	6.3
		24	7.9	12	3.7-13.5	6.8
		24.5	8.2	13	3.8-13.6	7.0
6	extensive everywhere.	26	9.6	15	4.0-14.5	7.4



One of the deficiencies of the above compensator is, in the case of long cables, the upper end cable tension does not clearly indicate the lower end cable (payload) behavior. Also in the case of motions with long periods, the acceleration—produced-tension changes may be too small to be detected to actuate the winch. Consequently, for these conditions, it is not possible to maintain the payload at a "fixed" position.

The motion compensator which is the topic of this thesis is basically the same as the above mentioned compensator, but with a different feedback technique. This thesis examines the system using the lower end cable tension (payload acceleration), payload velocity and displacement as the primary feedback. In this case, the cable handling the system follows the resulting ship motion more closely, and as a result, the payload suspended from the cable should remain "fixed" with reference to an earth datum level and a smaller transient cable tension should result.

Because of the limitation (particularly stability) on the overall gain of the control loop, it is not possible to maintain the payload absolutely stationary and the cable tension truly constant (the transient component zero). This thesis determines the possible limit of performance that can be expected from the proposed feedback system.

## CHAPTER II

MOTION OF MASSES LOCATED AT  
THE END OF A CABLE

The model shown in Figure 3 is used to derive the equation of motion of the payload in deep water and for further study in controlling the payload position. The corresponding block diagram of Figure 3 is shown in Figure 4.

1. Equations

The cable is assumed to act as a spring with spring constant  $K$ ; its mass (in the water),  $m$ , is assumed concentrated at a point at the end of the spring;  $m_1$  is the virtual mass [6,7] [A]\* of the payload in water ( $m_p$  mass of the payload); and  $C$  is the average viscous damping coefficient of the payload submerged in water.

The following vertical displacements are with respect to an inertial reference, unless otherwise specified.  $Z$  is the vertical component motion of the pulley axis  $Q$ ;  $X$  is the displacement of a point at the upper end of the cable with respect to the pulley axis;  $Y$  is the displacement of the upper end of the cable and  $P$  is the displacement of

\*Letters in brackets designate Appendix.

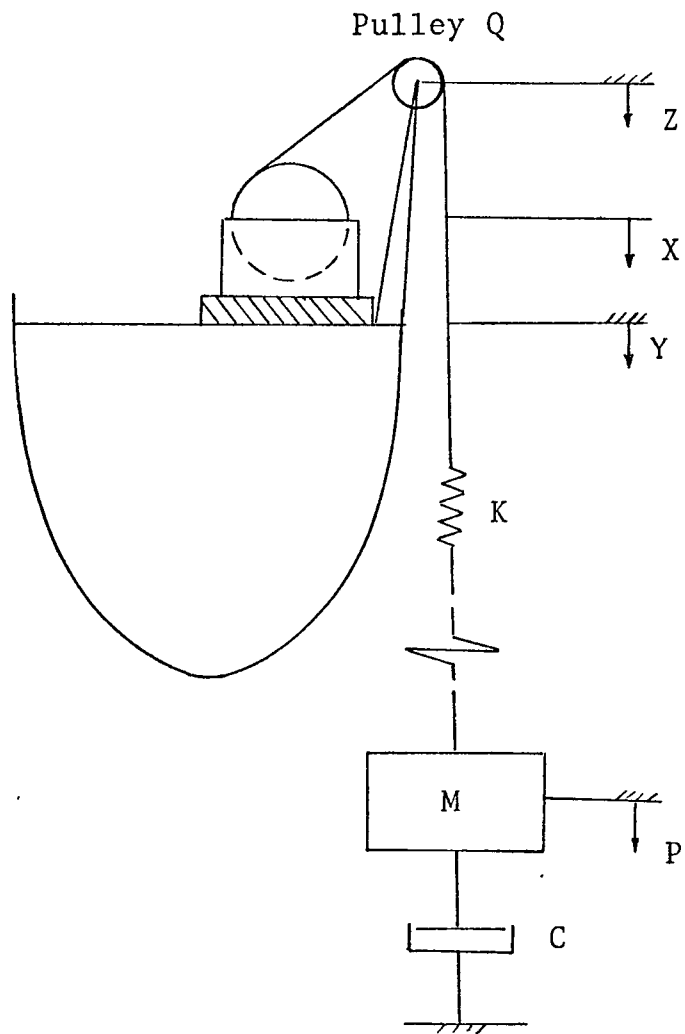


Figure 3. Vessel and Cable Model

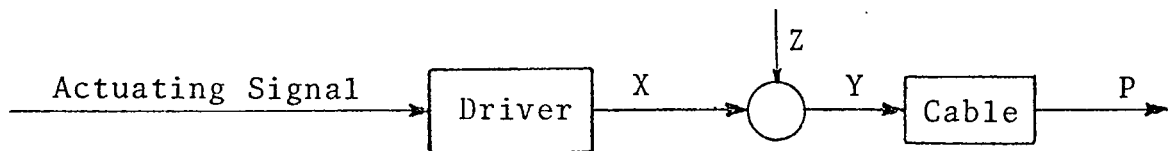


Figure 4. Vessel and Cable Block Diagram

the payload.

The transfer function of the cable, considering  $Y$  as the input and  $P$  as the output, can be obtained (Figure 5) [8]:

$$F = K(P - Y)$$

$$M = m + m_1$$

$$M \frac{d^2 P}{dt^2} = -C \frac{dP}{dt} - K(P - Y)$$

$$M \frac{d^2 P}{dt^2} + C \frac{dP}{dt} + KP = KY.$$

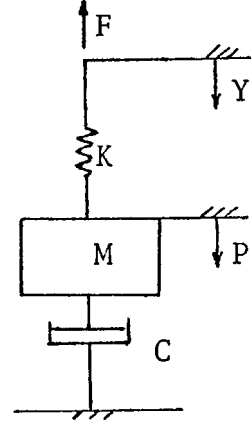


Figure 5. Cable Model

Taking the Laplace Transform, considering the initial conditions equal to zero and at the time under consideration that  $K$ ,  $C$  and  $M$  do not vary with the time, gives:

$$P(s) (MS^2 + CS + K) = KY(s),$$

so the transfer function relating  $Y(s)$  and  $P(s)$  becomes

$$G(s) = \frac{P(s)}{Y(s)} = \frac{K}{MS^2 + CS + K},$$

or

$$G(s) = \frac{P(s)}{Y(s)} = \frac{K/M}{S^2 + (C/M)S + K/M} \quad (1)$$

The values for K and C are calculated as follows:

K:

For a cable with the length L, cross sectional area A and modulus of elasticity E the elongation,  $\Delta L$ , for the load W is

$$\Delta L = \frac{W \cdot L}{A \cdot E} , \quad (2)$$

and for a spring (cable model) with spring constant K the length change,  $\Delta L$ , under the load W is

$$\Delta L = \frac{W}{K} . \quad (3)$$

Equating equations (2) and (3) gives the spring constant for a cable. Hence

$$K = \frac{A \cdot E}{L} . \quad (4)$$

C:

The drag force exerted on the payload during its displacement in the water is assumed to act as the force applied from a dashpot with average damping coefficient, C.

The drag force [9] for an object with cross sectional area  $A_p$  perpendicular to the direction of motion, moving with velocity V, in a fluid with density  $\rho$  is

$$F_D = \frac{1}{2} \rho C_D A_P V^2 , \quad (5)$$

$C_D$  is the drag coefficient which is a function of object shape and Reynold's number. In Table 4,  $C_D$  is shown for some objects for Reynold's numbers  $> 10^3$  [10].

The force applied by the dashpot is

$$F = CV . \quad (6)$$

The energy dissipated by the drag force for a certain payload displacement is equal to the energy dissipated by the equivalent dashpot; therefore,

$$\int_a^b F_D dy = \int_a^b F dy , \quad (7)$$

since

$$dy = V dt , \quad (8)$$

substitute (8) into (7), then,

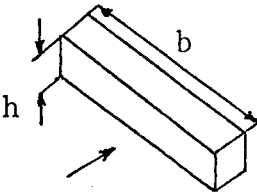



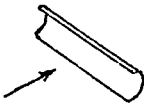
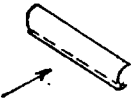
$$\int_{t_1}^{t_2} F_D V dt = \int_{t_1}^{t_2} F V dt . \quad (9)$$

Assuming a sinusoidal displacement,  $y$ , with amplitude  $Y$  and frequency  $\omega$  gives

$$y = Y \sin \omega t ,$$

TABLE 4

DRAG COEFFICIENT DATA FOR SELECTED  
OBJECTS ( $Re \geq 1000$ )

Object	Diagram	$C_D (Re \geq 1000)$	
Square Cylinder		$b/h = \infty$	2.05
		$b/h = 1$	1.05
Disc			1.17
Hemisphere (open end facing flow)			1.42
Hemisphere (open end facing downstream)			.38
C-section (open)			2.30
C-section (open)			1.2

and the payload velocity is

$$V = \omega Y \cos \omega t , \quad (10)$$

substituting (5), (6) and (10) into (9) gives

$$C = \frac{1}{2} \rho C_D A_P \omega Y \frac{\int_{t_1}^{t_2} \cos^3 \omega t dt}{\int_{t_1}^{t_2} \cos^2 \omega t dt} . \quad (11)$$

Let  $T$  be the period of payload oscillation ( $\omega = \frac{2\pi}{T}$ ) and

$$\begin{aligned} t_1 &= 0 \\ t_2 &= \frac{T}{4} , \end{aligned} \quad (12)$$

substituting (12) into (11) gives

$$C = \frac{4}{3\pi} \rho C_D A_P \omega Y . \quad (13)$$

## 2. Calculations

The Bode plot or frequency response curve of the cable transfer function relates the payload displacement (lower end of the cable) to motion of the upper end of the cable at different frequencies.

Transfer functions and the corresponding frequency response curves (Bode plots) of the cable for different



cases are shown in Figures 6 - 11.

The following parameters are the same for all cases:

$$A_p = 20 \text{ m}^2$$

$$\rho = 1,000 \text{ Kg/m}^3$$

$$d = 44 \text{ mm} \quad (\text{diameter of the cable})$$

$$\lambda = 8.1 \text{ Kg/m} \quad (\text{mass of the cable per unit length})$$

$$T = 5.7 \text{ sec}$$

$$\omega = 1.1 \text{ rad/sec}$$

$$m_1 = 2 m_p$$

As can be seen from the Bode plots, the motion can be amplified within the practical frequency range of the ship oscillation ( $.3 < \omega < 1.5 \text{ rad/sec}$ ), and in most of the cases, due to the natural frequency of the system, the highest amplification occurs in the critical frequency range ( $.5 < \omega < 1.2 \text{ rad/sec}$ ). In the case of a short cable (high spring constant) with a light payload (large safety factor), the ratio between the ship motion and the payload motion is approximately one within the practical frequency range of the ship oscillation; however, at the natural frequency of the system, this ratio is almost 3.75.

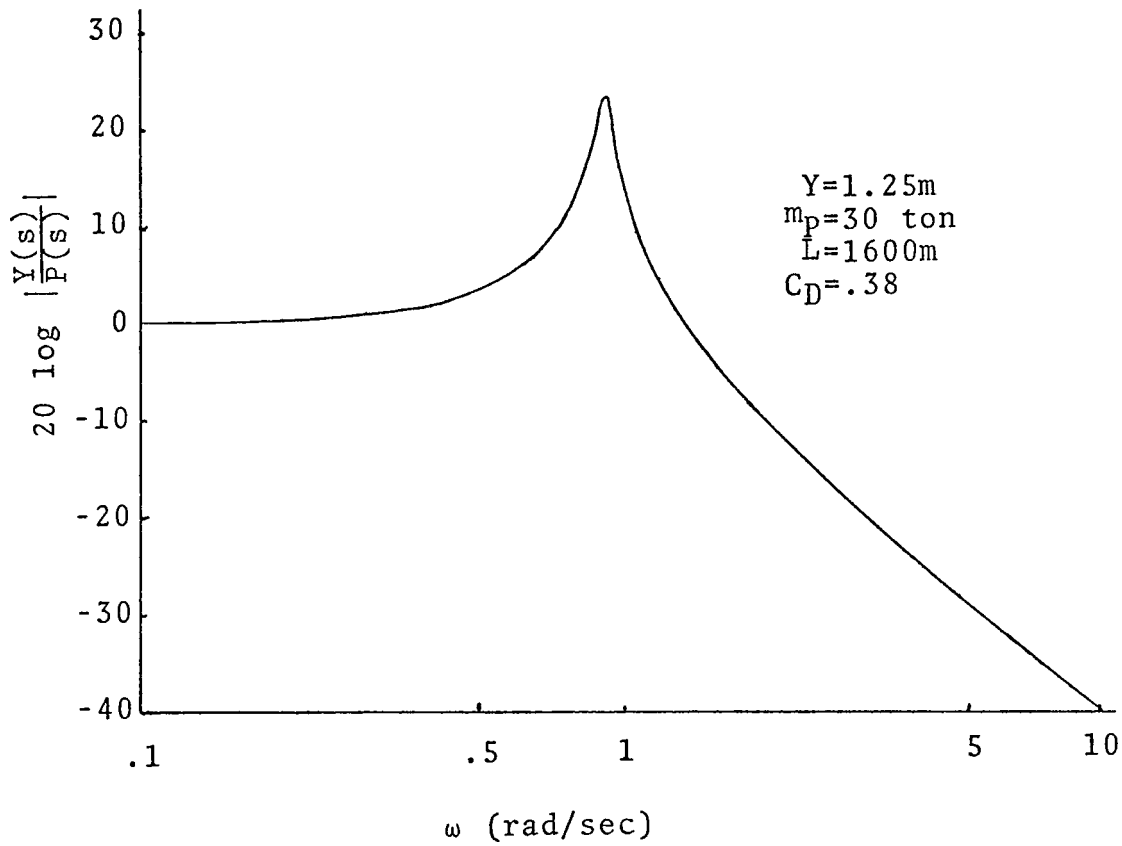


Figure 6. Frequency Response of the Cable (Bode Plot)

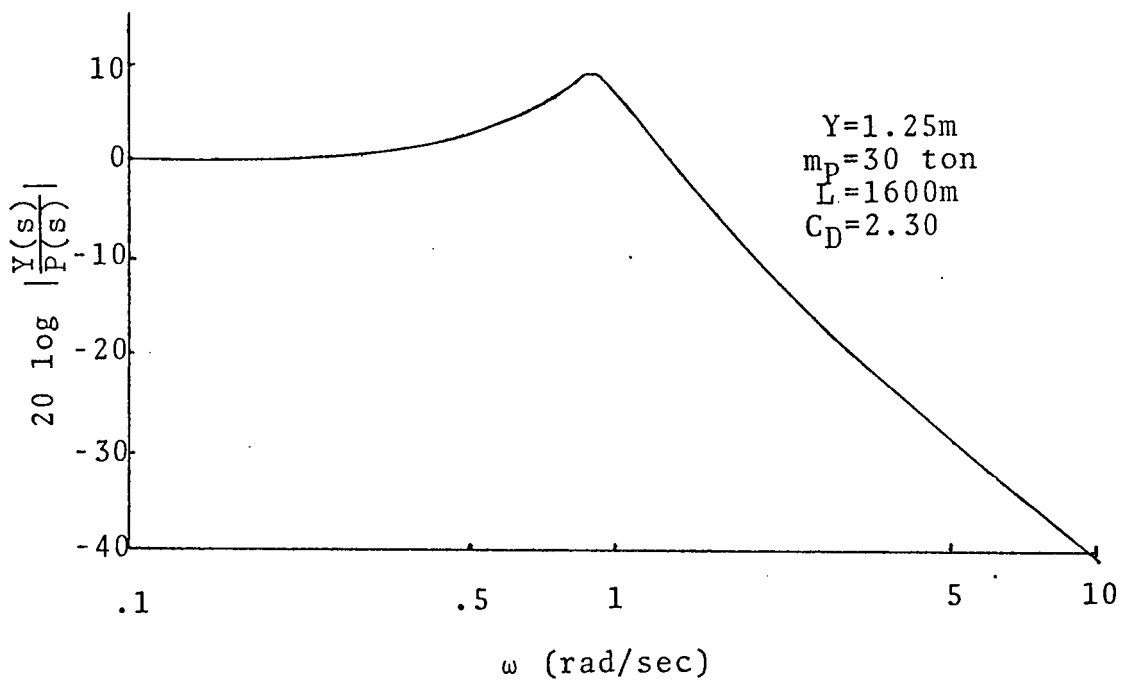


Figure 7. Frequency Response of the Cable (Bode Plot)

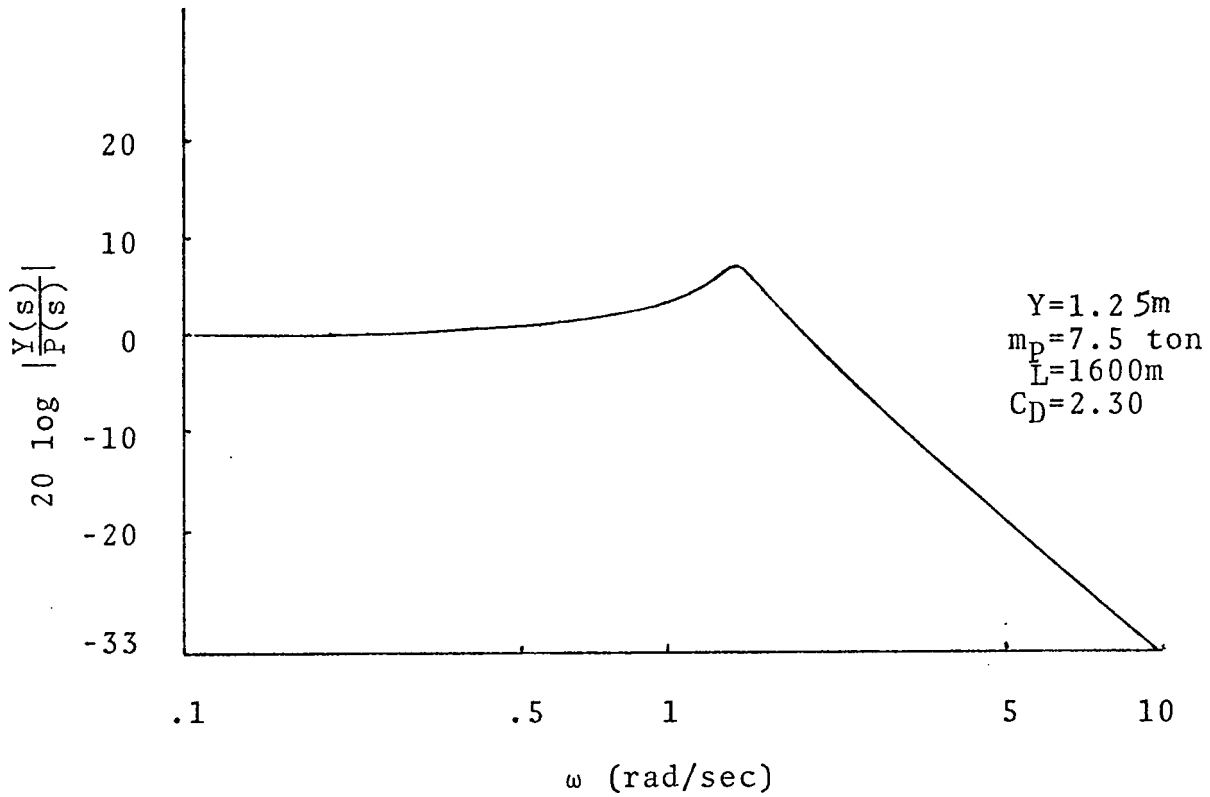


Figure 8. Frequency Response of the Cable (Bode Plot)

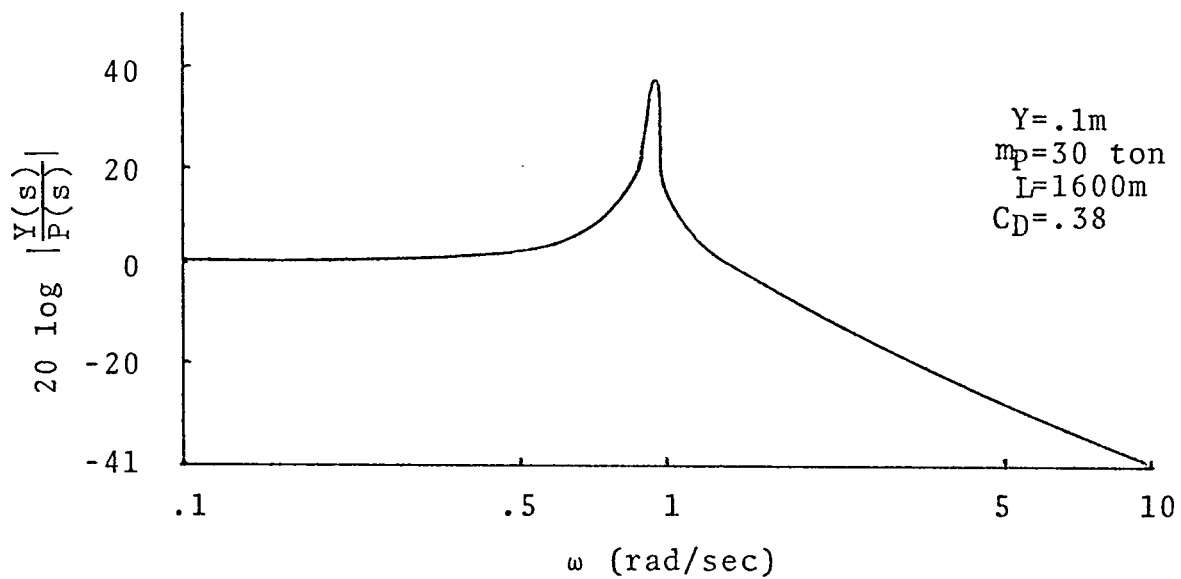


Figure 9. Frequency Response of the Cable (Bode Plot)

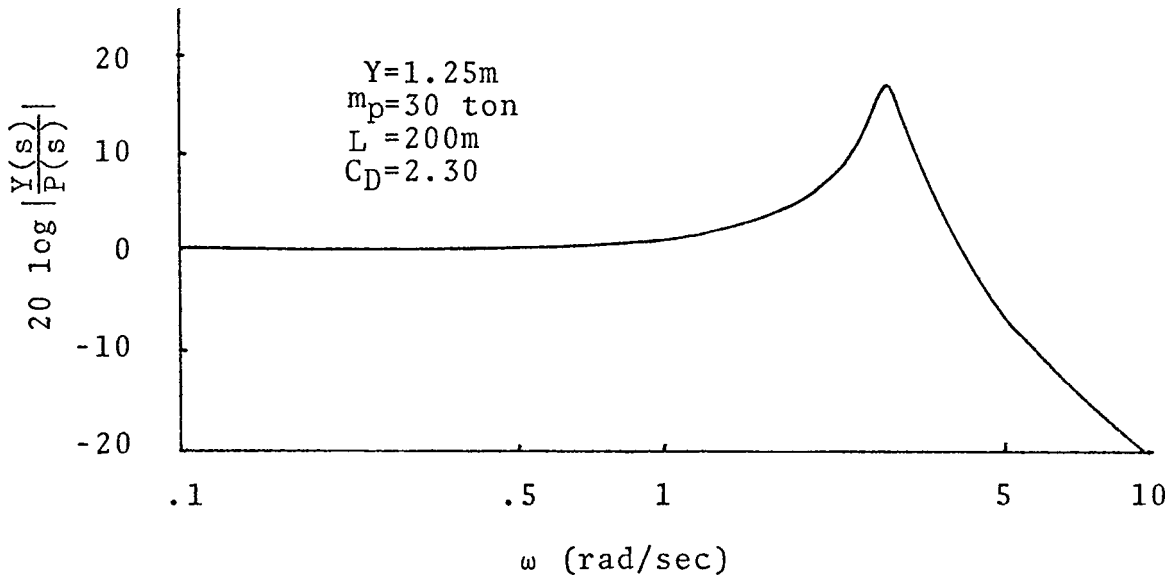


Figure 10. Frequency Response of the Cable (Bode Plot)

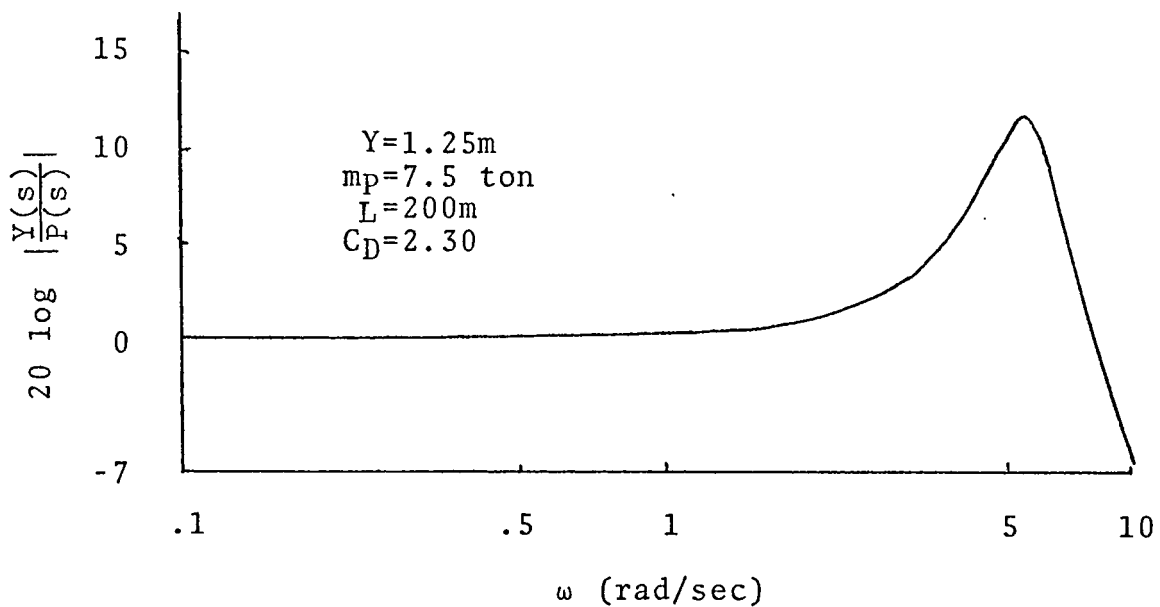


Figure 11. Frequency Response of the Cable (Bode Plot)

## CHAPTER III

## WINCH AND CABLE TRANSFER FUNCTIONS

1. Equations

If the tension in the upper end of the cable is  $F$  (Figure 5) and the effective radius of the winch drum (drum with cable lays) is  $r$ , then the developed torque on the drum shaft by  $F$  is:

$$T_D = F \cdot r$$

or

$$T_D = K(P-Y)r \quad (14)$$

It will be assumed that the winch shaft is connected to the drive shaft through a gearbox with the gear ratio  $n$ , the moment of inertia of the drum effective on the drum shaft is  $I_D$ , the coefficient of viscous friction between the drum shaft and a stationary reference (which would develop a torque proportional to the angular velocity) effective on the drum shaft is  $B_D$ , the moment of inertia of the gearbox effective on the gearbox input shaft is  $I_G$  and the coefficient of viscous friction of the gearbox on this shaft is  $B_G$ , so that the equivalent moment of inertia and coefficient of

viscous friction on the gearbox input shaft is:

$$I_T = I_G + \frac{I_D}{n^2} ,$$

and

$$B_T = B_G + \frac{B_D}{n^2} .$$

If  $\theta$  and  $\theta_1$  are angular displacements of the gearbox input shaft and the drum shaft respectively

$$\theta_1 = \frac{\theta}{n} \quad (15)$$

$$X = r\theta_1 \quad (16)$$

substituting (15) into (16) will give

$$\theta = \frac{Xn}{r} . \quad (17)$$

Hence the required torque on the gearbox input shaft can be determined as:

$$T_G = I_T \frac{d^2\theta}{dt^2} + B_T \frac{d\theta}{dt} - T_{DG} , \quad (18)$$

where  $T_{DG} = \frac{T_D}{n}$  is the equivalent of  $T_D$  on the input gearbox shaft.

Substituting (14) and (17) into (18) will give

$$T_G = I_T \frac{nd^2x}{rdt^2} + B_T \frac{ndx}{rdt} - K \frac{r}{n} (P - Y) . \quad (19)$$

Taking the Laplace Transform of (18) and considering the initial conditions equal to zero and  $I_T$ ,  $B_T$  and  $r$  to be time invariant will give

$$T_G(s) = (I_T S^2 + B_T S) \theta(s) - K [P(s) - Y(s)] r .$$

## 2. Block Diagram

Considering that

$$G(s) = \frac{Y(s)}{P(s)} = \frac{K}{MS^2 + CS + K} , \quad (20)$$

and

$$Y(s) = X(s) + Z(s) , \quad (21)$$

the corresponding block diagram shown in Figure 12 can be developed. Additional simplification provides the block diagram of Figure 13.

It should be noted that  $T_G$  can be supplied by one of several types of drive systems, i.e., electrical, mechanical, hydraulic or various combinations.

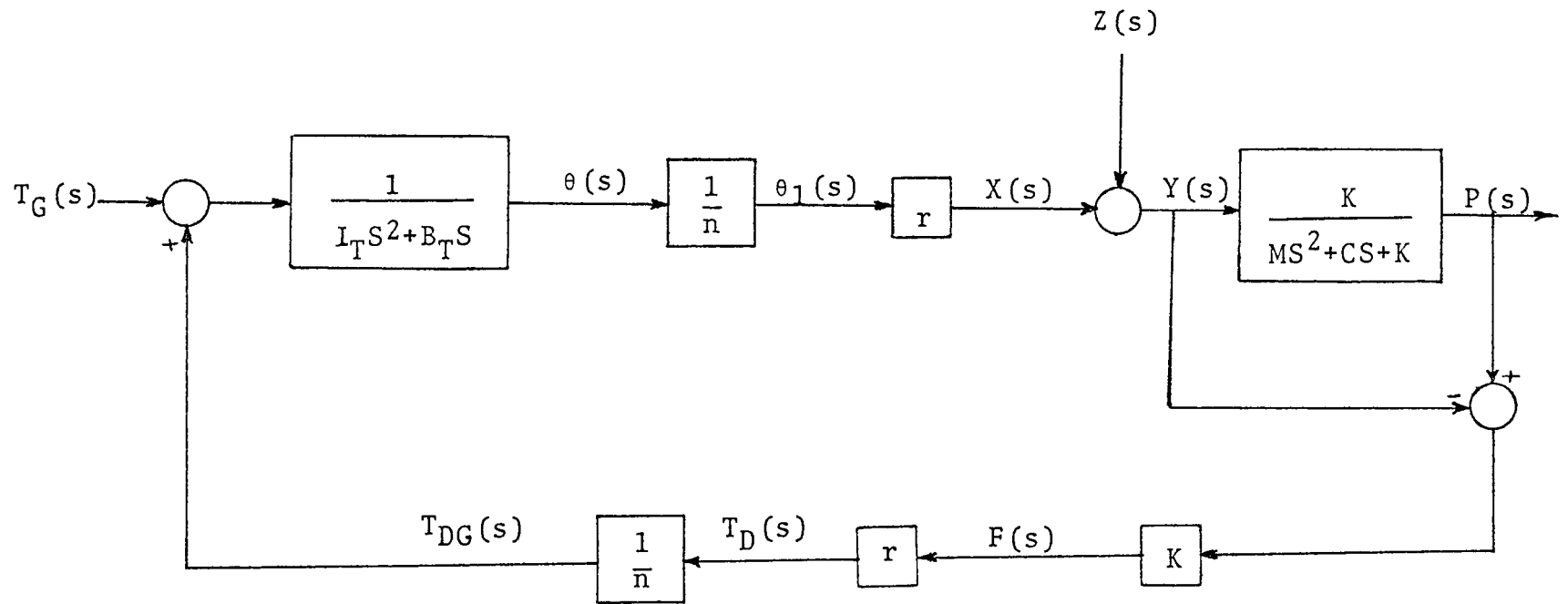


Figure 12. Winch and Cable Block Diagram



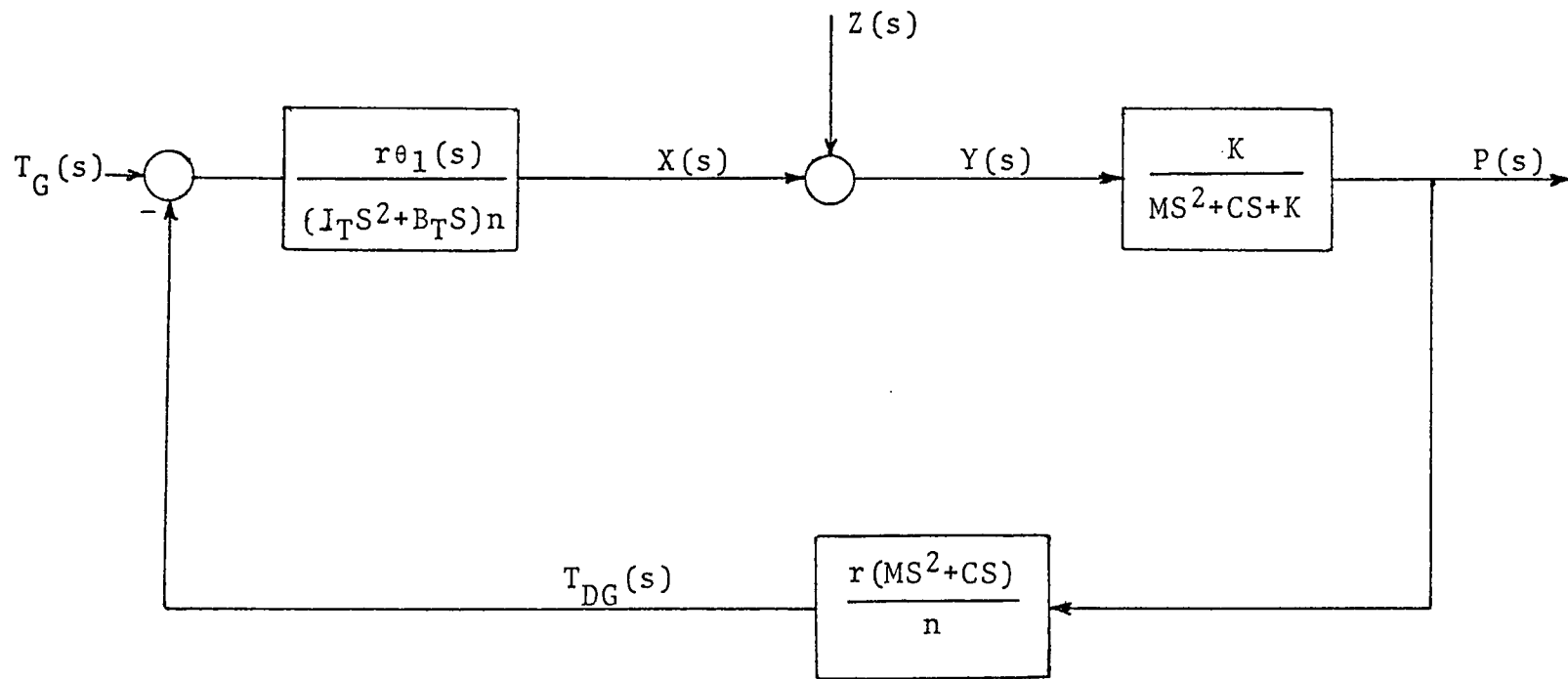


Figure 13. Simplification of Block Diagram Shown in Figure 12

## CHAPTER IV

OPEN LOOP SYSTEM PERFORMANCE  
(D-C ARMATURE CONTROL MOTOR DRIVING UNIT)

A D-C armature control motor is widely used as a winch drive and consequently the system in Figure 14 will be considered. In this system, the motor armature current is supplied by the voltage  $E_a$  and the motor is connected to the input shaft of the gearbox. The motor has an armature resistance  $R$  and an induction  $L'$ . The armature has a moment of inertia  $I_M$  and a coefficient of viscous friction  $B_M$ . The armature current is  $I'$  and the angular displacement of the shaft is  $\theta$  [11,12].

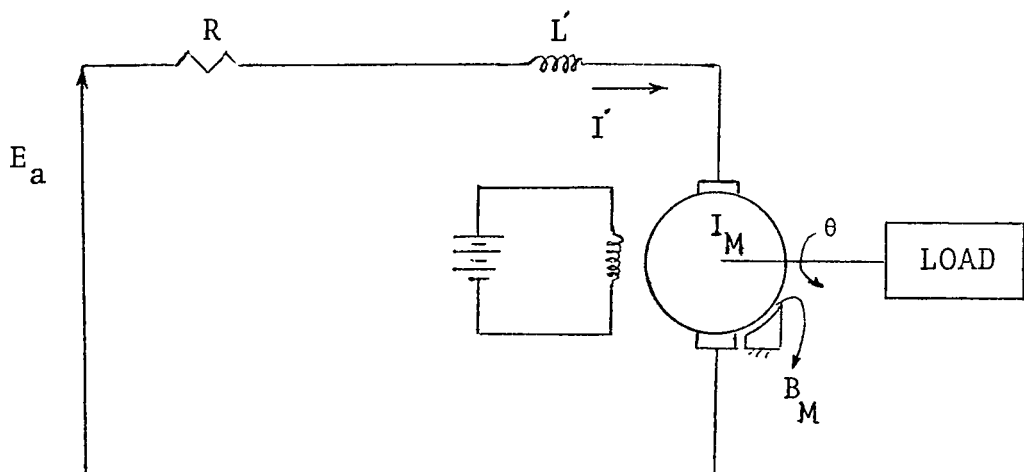


Figure 14. D-C Armature Control Motor

The motor counter emf is  $E_B = K_\omega \frac{d\theta}{dt}$ , where  $K_\omega$  is a constant for a specific motor. The torque developed by the motor is  $T_D = K_T I'$  where  $K_T$  is a constant for each particular motor.

Summing the torques for equilibrium gives:

$$T_D = I \frac{d^2\theta}{dt^2} + B \frac{d\theta}{dt} - T_{DG} , \quad (22)$$

where

$$I = I_M + I_G + \frac{I_D}{n^2} ,$$

and

$$B = B_M + B_G + \frac{B_D}{n^2} .$$

Let  $L' \approx 0$  (a reasonable assumption), then

$$E_a = RI' + E_B . \quad (23)$$

The back emf is given as

$$E_B = K_\omega \frac{d\theta}{dt} . \quad (24)$$

Taking the Laplace Transform of (22), (23) and (24) and combining these with (17), (20) and (21) gives

$$X(s) = \frac{K_T E(s)}{RD(s)} + \frac{KrP(s)}{nD(s)} - \frac{KrZ(s)}{nD(s)},$$

where

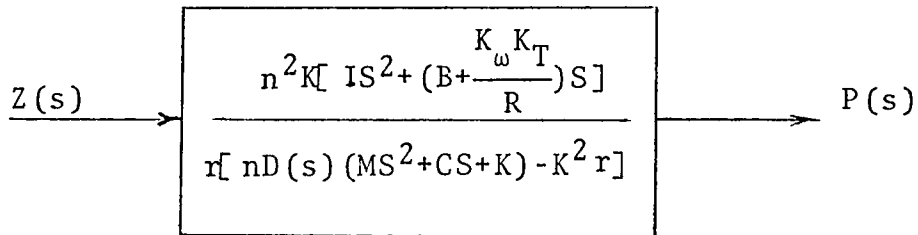
$$D(s) = \frac{n_r}{r} [IS^2 + (B + \frac{K_\omega K_T}{R})S + \frac{Kr^2}{n^2}] . \quad (25)$$

The corresponding open loop block diagram for this system is shown in Figure 15. This can be simplified to give the diagram in Figure 16.

NOTE: If the winch system shown in Figure 13 has the torque  $T_G$  supplied by a D-C armature control drive, the block diagram shown in Figure 17 results, which after simplification is exactly the same as the one shown in Figure 16, where  $T_G$ ,  $I_T$ ,  $B_T$  in Figure 13 will change to  $T_D$ ,  $I$  and  $B$  respectively.

From Figure 16, the following open loop transfer functions result.

When  $E_a = 0$ , then the relation between  $P$  and  $Z$  is:



Let

$$D'(s) = \frac{R}{n} [nD(s) (MS^2 + CS + K) - K^2 r] , \quad (26)$$

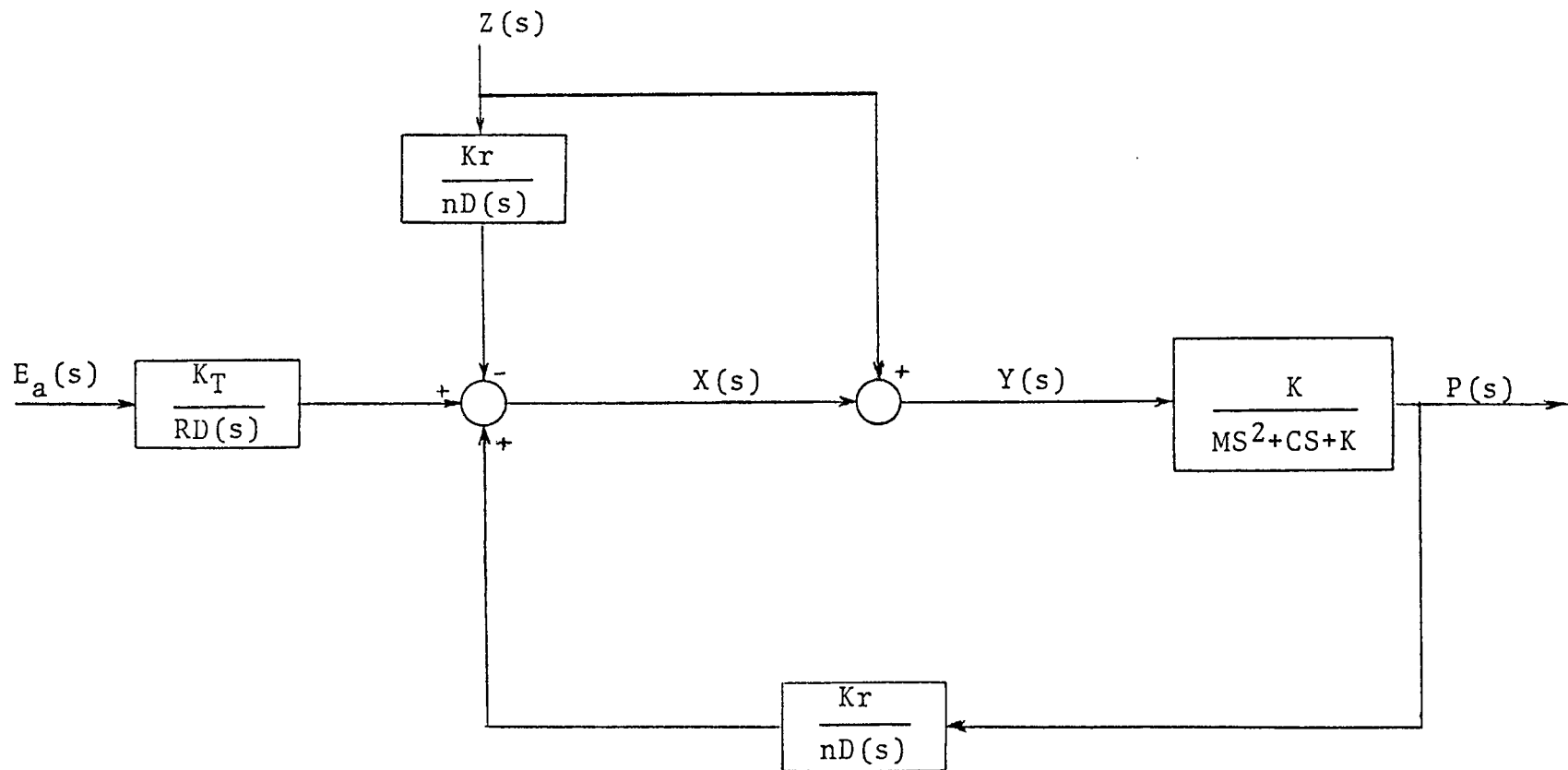


Figure 15. Open Loop Block Diagram of the System

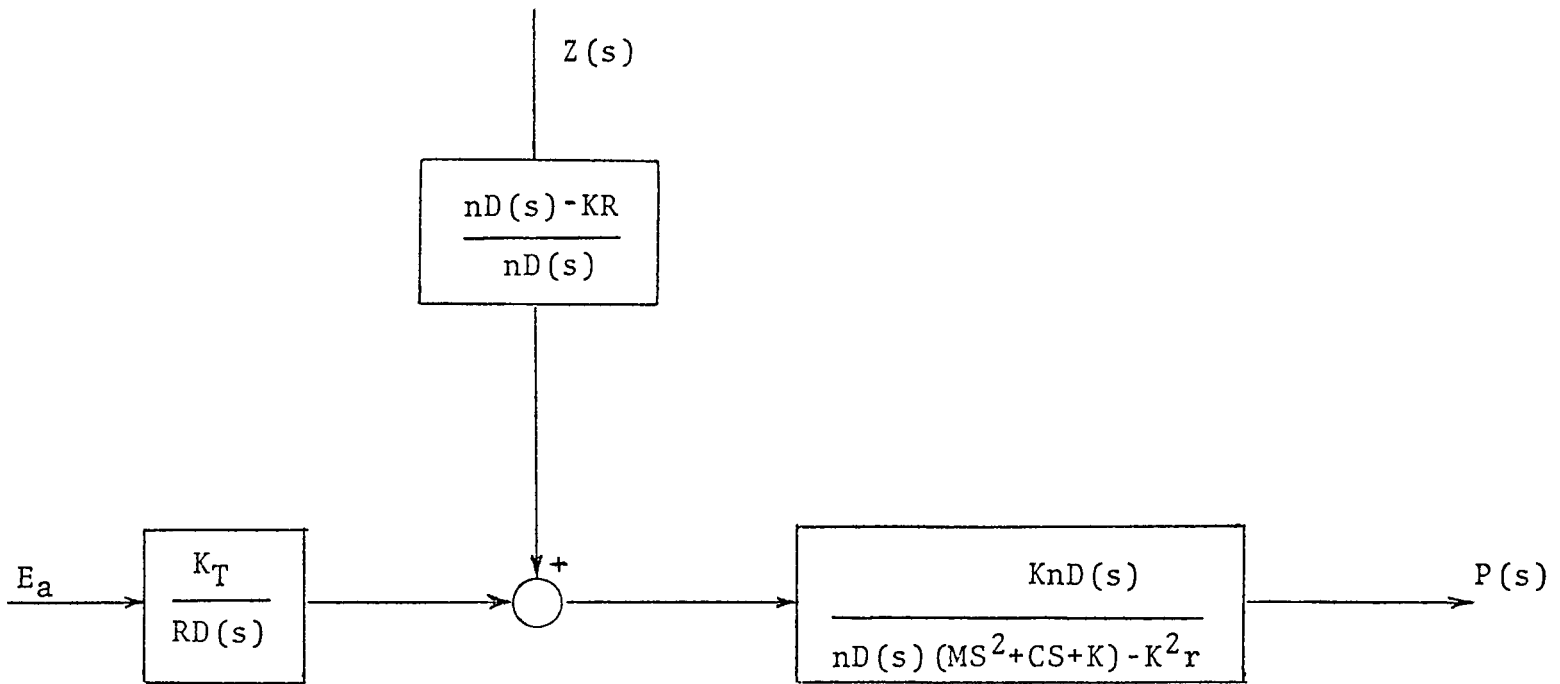


Figure 16. Simplification of Block Diagram Shown in Figure 15

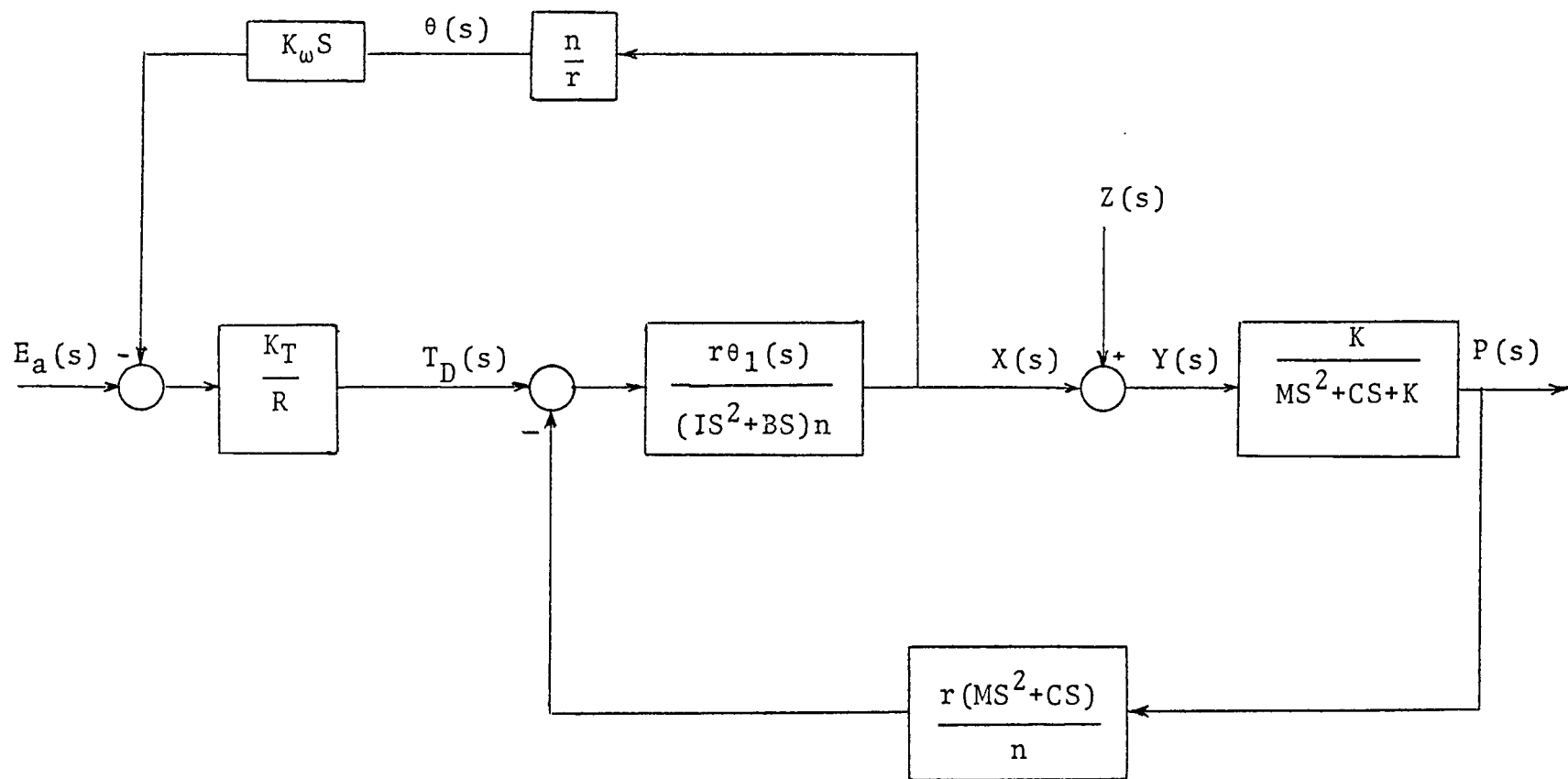


Figure 17. Open Loop Block Diagram of the System

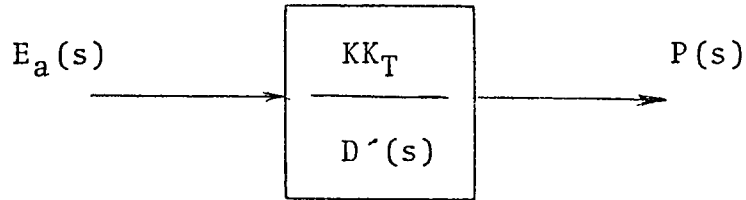
then, substituting (25) into (26) will give

$$D'(s) = \frac{Rn}{r} \left[ IMS^4 + \left[ IC + \left( B + \frac{K_\omega K_T}{R} \right) M \right] S^3 + \left[ \frac{MKr^2}{n^2} + C \left( B + \frac{K_\omega K_T}{R} \right) + KI \right] S^2 + K \left[ B + \frac{K_\omega K_T}{R} + \frac{Cr^2}{n^2} \right] S \right] . \quad (27)$$

So that,

$$T^*(s) = \frac{P(s)}{Z(s)} = \frac{nKR \left[ IS^2 + \left( B + \frac{K_\omega K_T}{R} \right) S \right]}{rD'(s)} . \quad (28)$$

When  $Z = 0$ , then the relation between  $P$  and  $E_a$  is:



So that,

$$T_1^*(s) = \frac{P(s)}{E(s)} = \frac{KK_T}{D'(s)} . \quad (29)$$



## CHAPTER V

## CLOSED LOOP SYSTEM PERFORMANCE

From the data shown in Chapter I, the need for motion compensators is apparent and by considering the cable's role in payload motion (Chapter II), it can be concluded that for efficient compensation, feedback signals should be transmitted from the lower end of the cable.

It is assumed that feedback signals can be obtained from the lower end of the cable (this is a realistic assumption). Summing these signals with the control voltage gives the block diagram shown in Figure 18.

In this figure,  $H(s)$  is a general second order polynomial in  $S$ :

$$H(s) = aS^2 + a_1S + a_2 \quad (30)$$

It should be noted that  $A$ ,  $a$ ,  $a_1$  and  $a_2$  are constants and can be identified as follows:

$A$  is the voltage-amplifier gain, and  $a$ ,  $a_1$  and  $a_2$  are the coefficients or transducer "gains" of the acceleration, velocity and displacement signals respectively.

For  $E_G = 0$ , the relationship between  $P$  and  $Z$  becomes as shown in Figure 19.

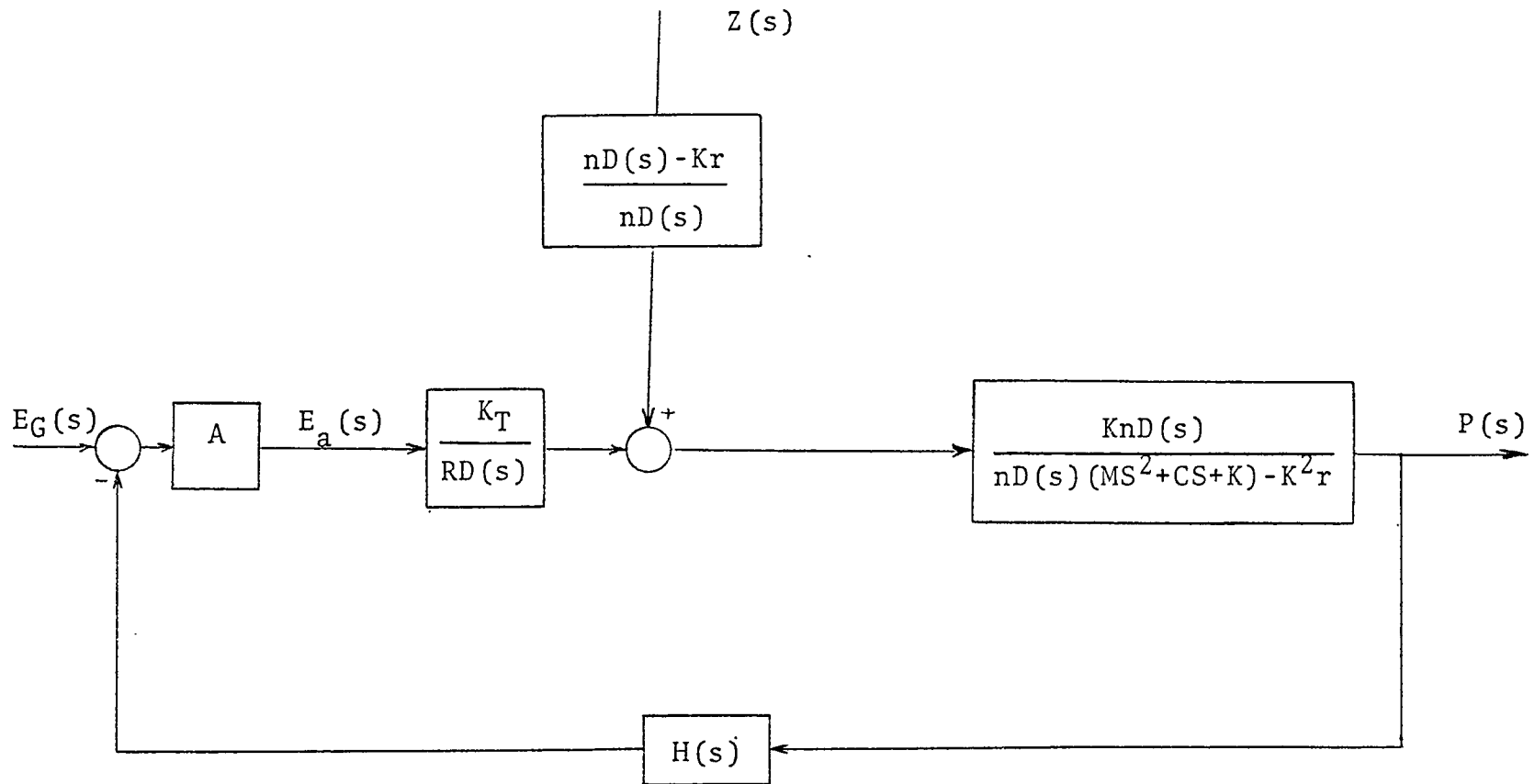


Figure 18. Closed Loop Block Diagram of the System

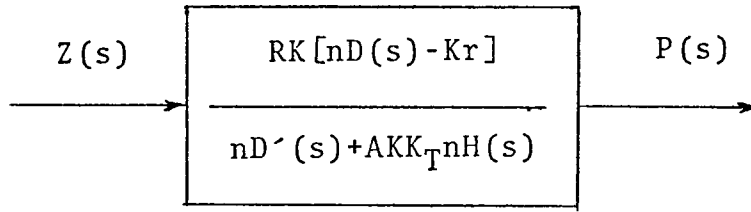


Figure 19. Relationship between Ship Motion and Payload Motion

Figure 19 shows the block diagram of interest. This is the relationship and transfer function between the lower-cable-end and the ship motion. This transfer function provides the response of the lower-cable-end that results from the ship motion as the driving function.

The relationship between  $P$  and  $Z$  is

$$T(s) = \frac{P(s)}{Z(s)} = \frac{RK[nD(s) - Kr]}{nD'(s) + AKK_T H(s)R} \quad (31)$$

Substituting (25), (26) and (30) into (31) gives:

$$T(s) = \frac{P(s)}{Z(s)} = \frac{\frac{K}{M}S^2 + (\frac{KB}{IM} + \frac{KK_\omega K_T}{IMR})S}{S^4 + [\frac{C}{M} + \frac{B}{I} + \frac{K_\omega K_T}{RI}]S^3 + [\frac{Kr^2}{In^2} + \frac{CB}{IM} + \frac{CK_\omega K_T}{IMR} + \frac{K}{M} + \frac{rKK_TAa}{nRIM}]S^2 + [\frac{KB}{IM} + \frac{KK_\omega K_T}{RIM} + \frac{CKr^2}{IMn^2} + \frac{rKK_TAa_1}{nRIM}]S + \frac{rKK_TAa_2}{nRIM}} \quad (32)$$

Now the final value theorem for a function and its Laplace transform is expressed as:

$$\lim_{t \rightarrow \infty} f(t) = \lim_{s \rightarrow 0} sF(s) \quad [13].$$

Applying this theorem in equation (32), considering  $Z(t)$  (ship motion) as a step change,  $Z(t) = Z u(t)$ , it can be seen that

$\lim_{t \rightarrow \infty} P(t) = 0$  [12] which means the final displacement of the payload

is zero. While a step change is unrealistic, it does provide an insight of the behavior of the system for very low frequency changes in amplitude such as tidal changes or long period swells.

Appropriate values for  $A$ ,  $a$ ,  $a_1$  and  $a_2$  in equation (32) are chosen that will result in a stable system that will give a satisfactory outputs (payload motions) for practical inputs (ship motions).

An important point to be noted is that the values of  $A$ ,  $a$ ,  $a_1$  and  $a_2$  do not need to be held to close tolerance. This insensitivity greatly reduces the practical difficulties of transmitting the required feedback signals. Calculations that indicate these properties are shown in Chapter VIII.

For  $Z = 0$ , the transfer function between  $P$  and  $E_G$  is:

$$T_1(s) = \frac{P(s)}{E_G(s)} = \frac{\frac{AKK_T r}{nRIM}}{S^4 + \left[ \frac{C}{M} + \frac{B}{I} + \frac{K_\omega K_T}{RI} \right] S^3 + \left[ \frac{Kr^2}{IN^2} + \frac{CB}{IM} + \frac{CK_\omega K_T}{RIM} + \frac{K}{M} \right] S^2 + \left[ \frac{KB}{IM} + \frac{KK_\omega K_T}{RIM} + \frac{CKr^2}{IMn^2} + \frac{AKK_{Tra1}}{nRIM} \right] S + \frac{AKK_{Tra2}}{nRIM}}$$

(33)

## CHAPTER VI

## WINCH CONTROL SYSTEM MOTION REQUIREMENTS

Using the relationship expressed in Figure 15 and applying feedback from P gives the block diagram shown in Figure 20. In this figure, A and H(s) have the same definitions as indicated in Chapter V. After simplification, the simple block diagram shown in Figure 21 is obtained ( $E_G = 0$ ).

The transfer function can be written as:

$$T_2(s) = \frac{X(s)}{Z(s)} = - \frac{\left[ \frac{Kr^2}{In^2} + \frac{AKK_{Tra}}{nRIM} \right] s^2 + \left[ \frac{CKr^2}{IMn^2} + \frac{AKK_{Tra1}}{nRIM} \right] s + \frac{AKK_{Tra2}}{nRIM}}{s^4 + \left[ \frac{C}{M} + \frac{B}{I} + \frac{K_\omega K_T}{RI} \right] s^3 + \left[ \frac{Kr^2}{In^2} + \frac{CB}{IM} + \frac{CK_\omega K_T}{RIM} + \frac{K}{M} \right] s^2 + \left[ \frac{KB}{IM} + \frac{KK_\omega K_T}{RIM} + \frac{CKr^2}{IMn^2} + \frac{AKK_{Tra1}}{nRIM} \right] s + \frac{AKK_{Tra2}}{nRIM}} \quad (34)$$

From the transfer function, it can be seen that X and Z have opposite signs. This is as expected since when Pulley Q is going up, the winch should pay out the cable and when the pulley A is coming down, the winch should haul in the cable.

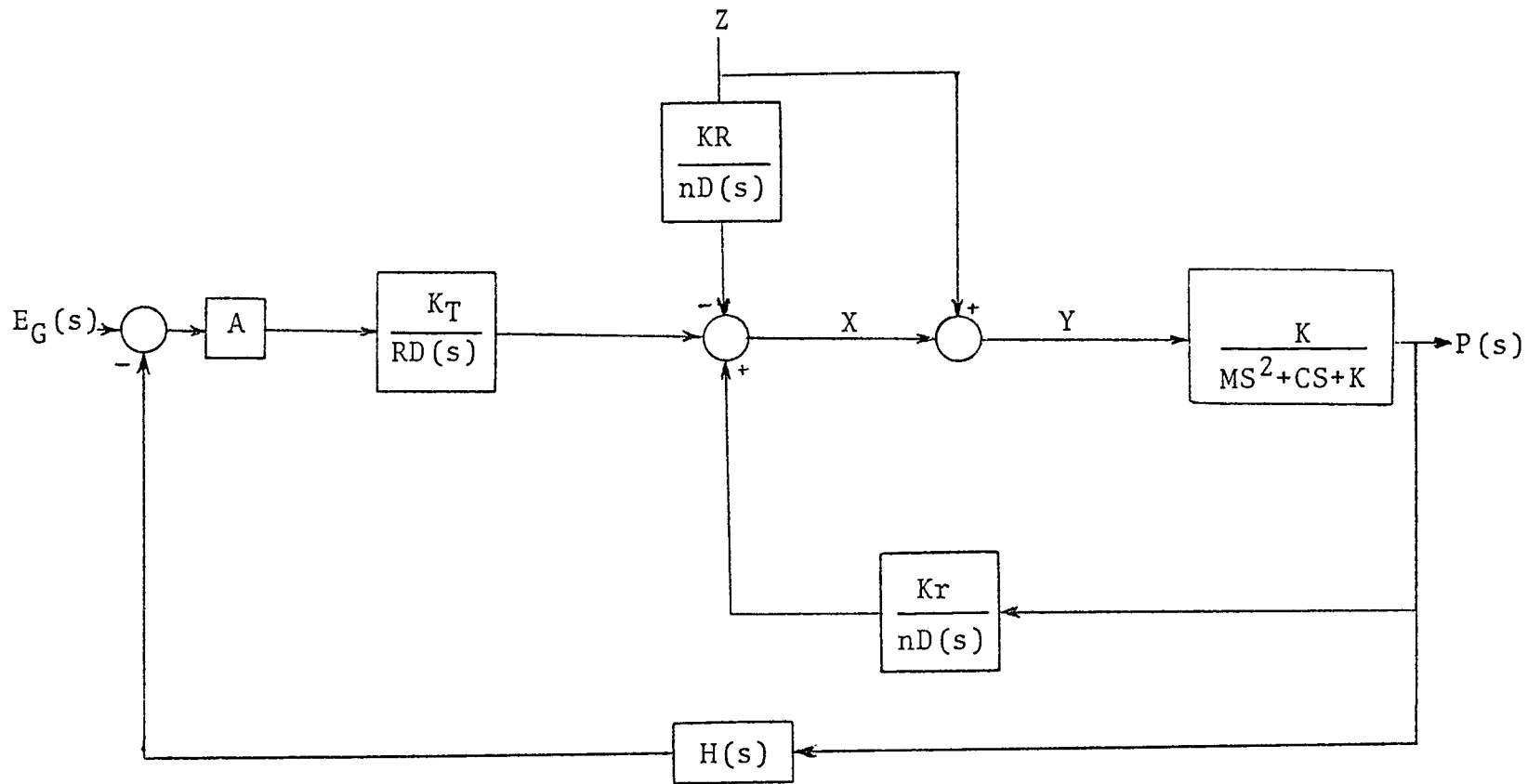


Figure 20. Closed Loop Block Diagram of the System

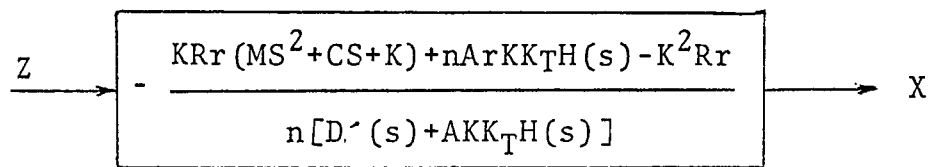


Figure 21. Relationship between Ship Motion and Drum Motion



## CHAPTER VII

## SHIP RESPONSE IN HEAVE

To find the ship response in heave and design the components of the control system, a fully developed-sea generated by a 20 knot wind is considered. For this sea state:

$$H_S = \text{significant wave height} = 2.5 \text{ m}$$

$$T_S = \text{significant period} = 8.1 \text{ sec}$$

Using the technique outlined in Appendix B [14] for finding the wave spectrum, the frequency spectrum shown in Figure 23 results. The corresponding figures are shown in Table 5.

The values used are:

$$\bar{H} = .625H_S = 1.52 \text{ m}$$

$$\bar{T} = .9T = 7.29 \text{ sec}$$

$$(\bar{H})^2 \bar{T} = 16.93 \text{ m}^2\text{-sec}$$

It should be noted that in this frequency-spectrum,  $\omega$  is in rad/sec.

The heave response of a medium-sized typical-hulled vessel used for offshore operations is shown in Figure 22 and Table 5.

The ship response in heave due to the assumed wave spectrum can be obtained by the following technique [15].

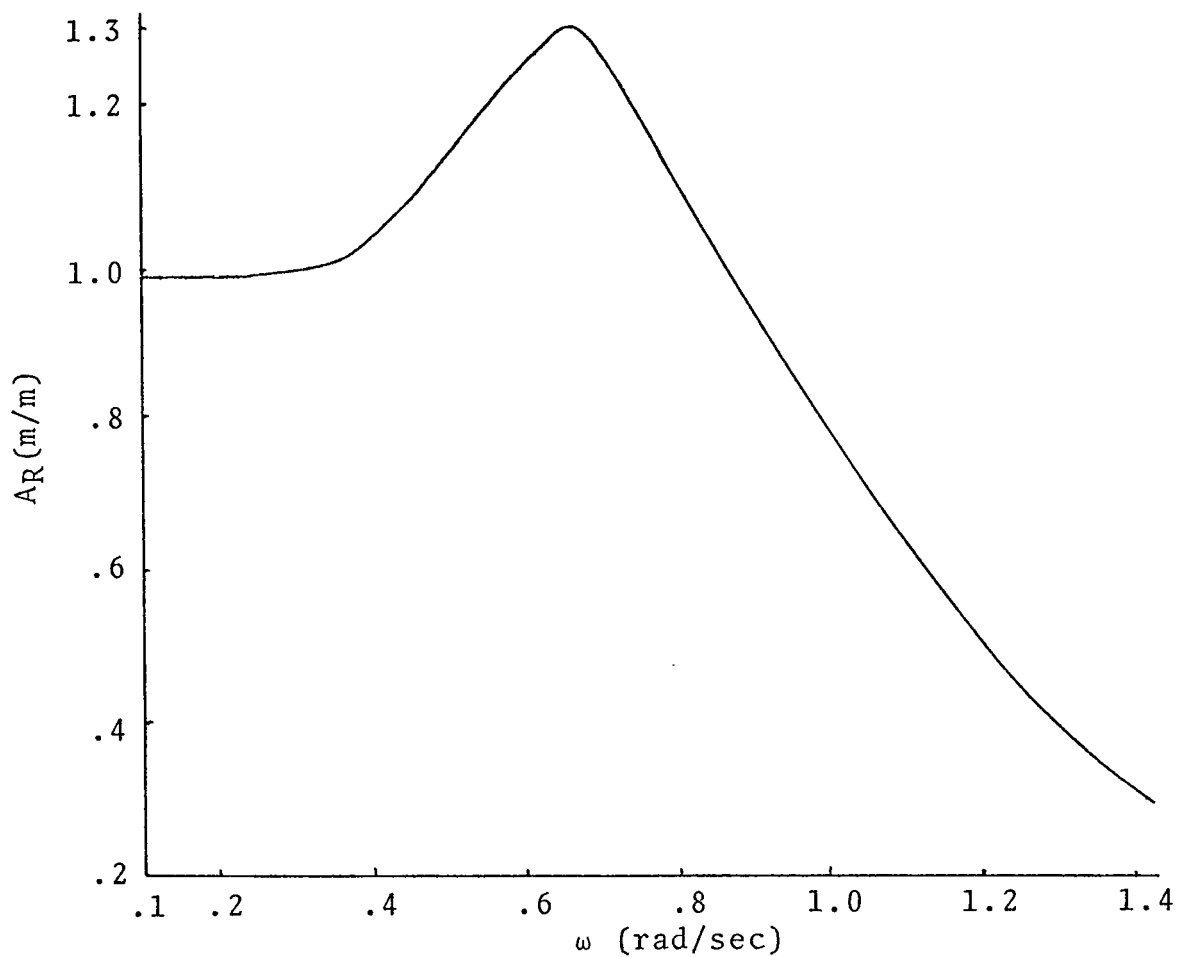


Figure 22. Heave Response

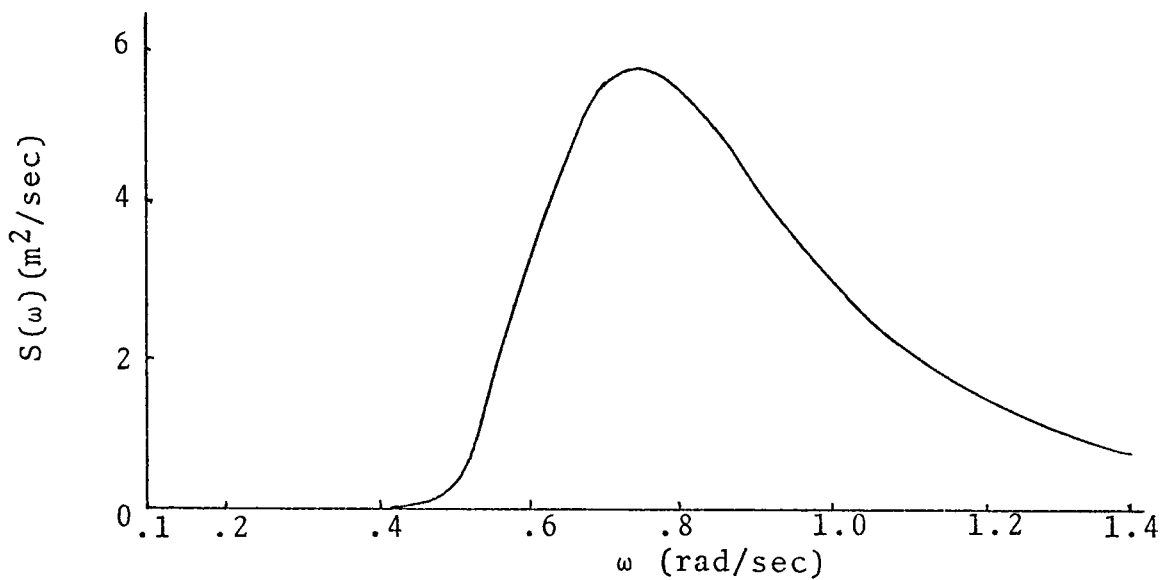


Figure 23. Frequency Spectrum

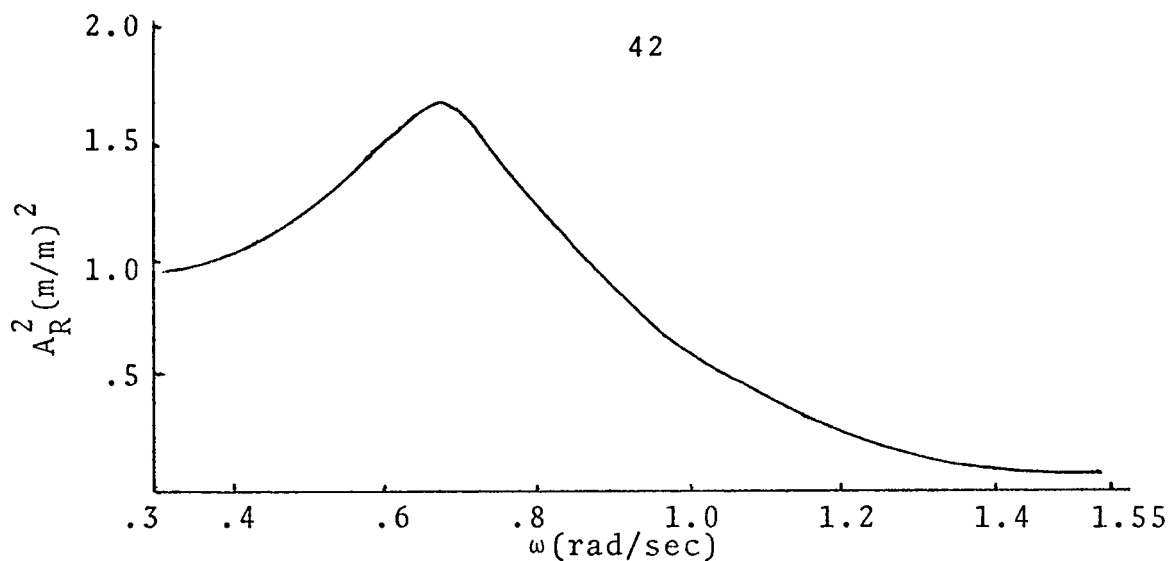


Figure 24. Heave Amplification Operator

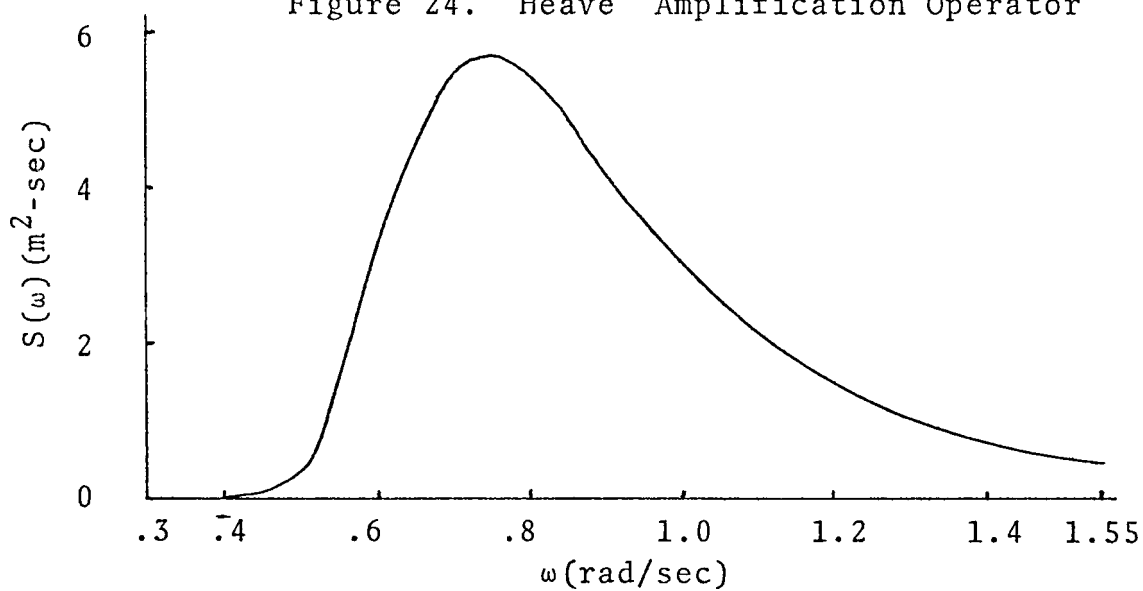


Figure 23. Frequency Spectrum (repeated)

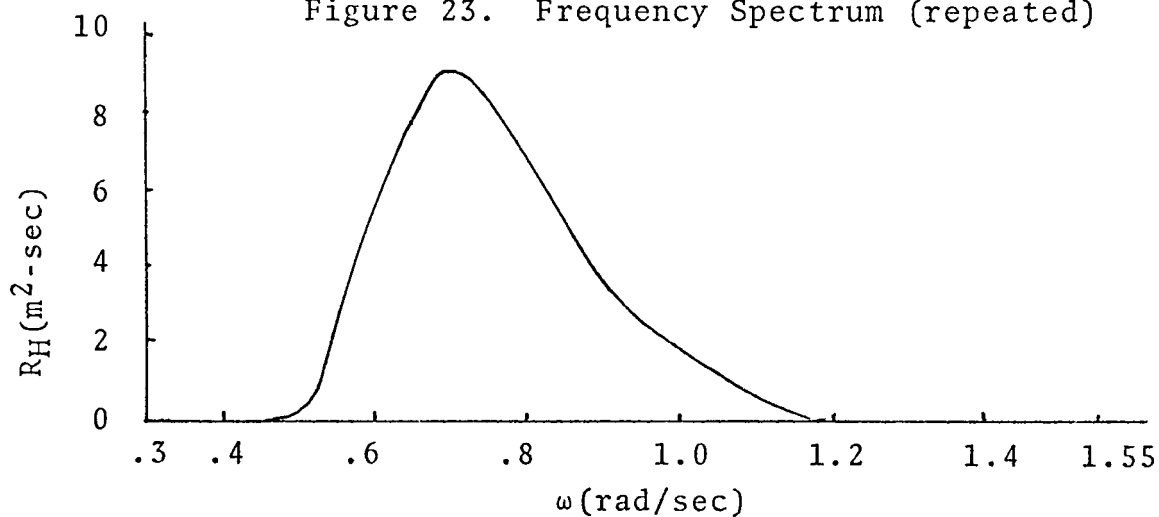


Figure 25. Ship Response in Heave

TABLE 5

## SHIP RESPONSE IN HEAVE

$\omega$ (rad/sec)	$A_R$ (m/m)	$A_R^2$ (m/m) <sup>2</sup>	$S(\omega)$ (m <sup>2</sup> -sec)	$R_H$ (m <sup>2</sup> -sec)
.34	.985	.97	0	0
.43	1.05	1.1	.006	.0066
.47	1.1	1.21	.125	.15
.52	1.17	1.37	.655	.9
.56	1.20	1.44	1.91	2.75
.60	1.23	1.51	3.34	5.05
.65	1.29	1.66	4.77	7.92
.69	1.29	1.66	5.44	9.05
.73	1.23	1.51	5.74	8.68
.78	1.15	1.32	5.58	7.37
.86	1	1	4.71	4.71
.94	.85	.72	3.61	2.61
1.03	.75	.56	2.69	1.51
1.12	.60	.36	1.98	.713
1.21	.50	.25	1.44	.36
1.29	.40	.16	1.06	.17
1.38	.35	.12	.80	.1
1.46	.32	.10	.6	.06
1.55	.26	.07	.46	.03

Let

$A_R$  = Heave amplitude/wave amplitude (m/m)

$S(\omega)$  = Frequency spectrum ( $m^2$ -sec)

$R_H$  = Ship response in heave due to the assumed wave  
spectrum ( $m^2$ -sec)

So,

$$R_H = (A_R)^2 S(\omega)$$

Table 5 and Figure 25 show the ship response in heave.

## CHAPTER VIII

CALCULATIONS FOR CHOOSING THE COMPONENTS OF THE  
WINCH-SYSTEM AND THE CONTROL SYSTEM1. Winch System

## a. Winch

Model 1000 American Hoist. Its specifications in metric unit are shown in Table 6.

## b. Drive Unit

Motor Model GE-752 powered by Generator Model GT-606. The motor has the following specifications (the symbols are the ones used in Chapter IV).

$$L' \approx 0$$

$$R = .074 \text{ ohm}$$

$$K_{\omega} = K_T = 5.8 \text{ volt/amp} \quad (1 \text{ volt/amp} = 1 \text{ nt-m/rad/sec})$$

$$I_M = 98 \text{ Kg-m}^2$$

The speed-torque and speed-horsepower curves for the motor are shown in Figure 26.

## c. Other Specifications of the Winch-System

Based on 1200 RPM motor speed and the maximum required linear velocity of the winch drum (for the sea-state under consideration), a gearbox with the gear ratio 37 is chosen.

TABLE 6

## MODEL 1000 AMERICAN HOIST SPECIFICATIONS

Standard .826 m Dia. x 1.89 m Long			
Rope Size mm	Layer	Layer Pitch Dia. m	Rope on Drum m
44	1	.87	109
	2	.95	228
	3	1.02	357
	4	1.10	495
	5	1.17	642
	6	1.25	799
	7	1.33	966
	8	1.40	1142
	9	1.48	1328
	10	1.56	1523
	11	1.63	1728
	12	1.71	1942
	13	1.78	2166

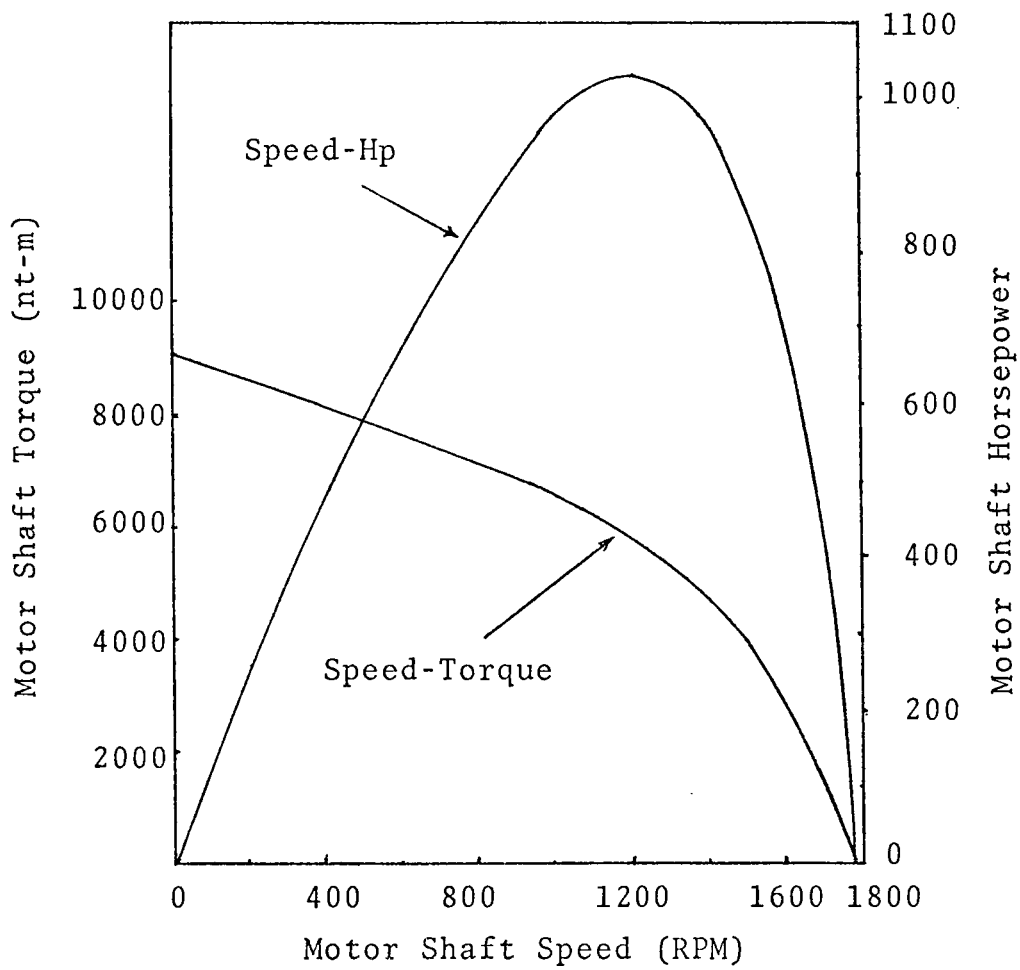


Figure 26. GE-752 Motor Curves



The moment of inertia of the drum,  $\frac{I_D}{n^2}$ , is almost negligible and  $I_G = 22 \text{ Kg-m}^2$ , so

$$I = I_M + I_G = 120 \text{ Kg-m}^2 .$$

To find the coefficient of viscous friction, B (assumed to be constant), it is assumed that 1% of the power of the drive unit is applied to overcome frictional forces; hence B can be determined as follows:

$$HP = B \left( \frac{d\theta}{dt} \right)^2$$

$$.01 \times 100 = B \left( \frac{1200}{9.55} \right)^2 \quad (9.55 \text{ RPM} = 1 \text{ rad/sec})$$

$$B = .47 \text{ nt-m/rad/sec}$$

## 2. Control System

In choosing the gains A, a,  $a_1$  and  $a_2$ , the following points should be considered:

1. The practical performance of the system should be fulfilled.
2. The transfer function  $T(s) = \frac{P(s)}{Z(s)}$ ; (32) (payload motion/ship motion) should have a magnitude much less than one and  $T_2(s) = \frac{X(s)}{Z(s)}$ ; (34) (drum required motion/ship motion) should have a magnitude about one where the wave spectrum has the maximum energy ( $.5 < \omega < 1.2 \text{ rad/sec}$ ).
3. The time response of the system to a sinusoidal input (wave approximation) should be fairly fast.

Considering the above discussion, a suboptimization for the worst case of the payload mass and cable length (highest motion amplification), studied in Chapter II will result in the following values:

$$A = 200$$

$$a = 50$$

$$a_1 = 100$$

$$a_2 = 100$$

Table 7 shows the ratio between the payload and the ship motion and the ratio between the drum and the ship motion for several different frequencies in the practical frequency range of the ship motion. In addition, the table also indicates the frequencies for which the above ratios have their maximum values. The corresponding frequency responses (Bode plots) are shown in Figures 27 and 28.

Applying the data and the technique explained in Chapter VII, the frequency-spectrum for payload motion resulting from heave motion before and after compensation is obtained (Figures 29 and 30 and Tables 8 and 9).

Figure 31 shows the compensated payload motion for a unit sinusoidal input (approximate ship motion) for three different frequencies.

Figure 32 represents the sensitivity test for 10% increase in the values of  $a$ ,  $a_1$  or  $a_2$ . As it can be seen, the performance of the system shows little change.

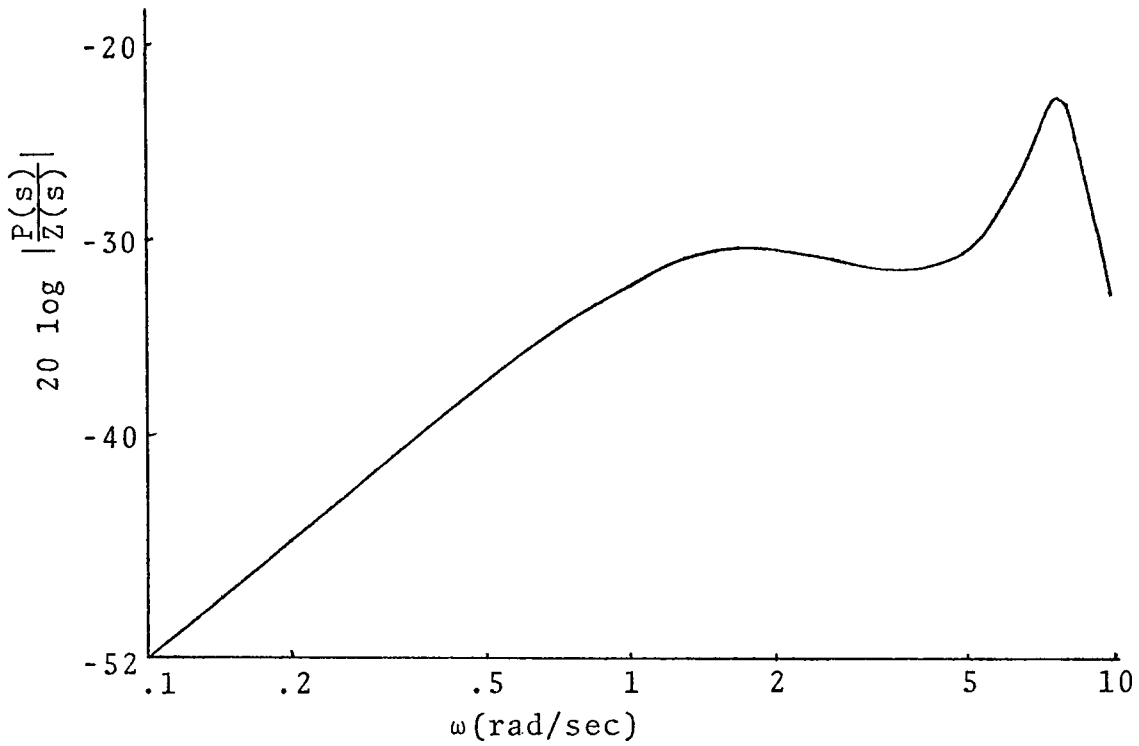


Figure 27. Frequency Response of Payload Motion  
With Respect to Ship Motion  
(Bode Plot)

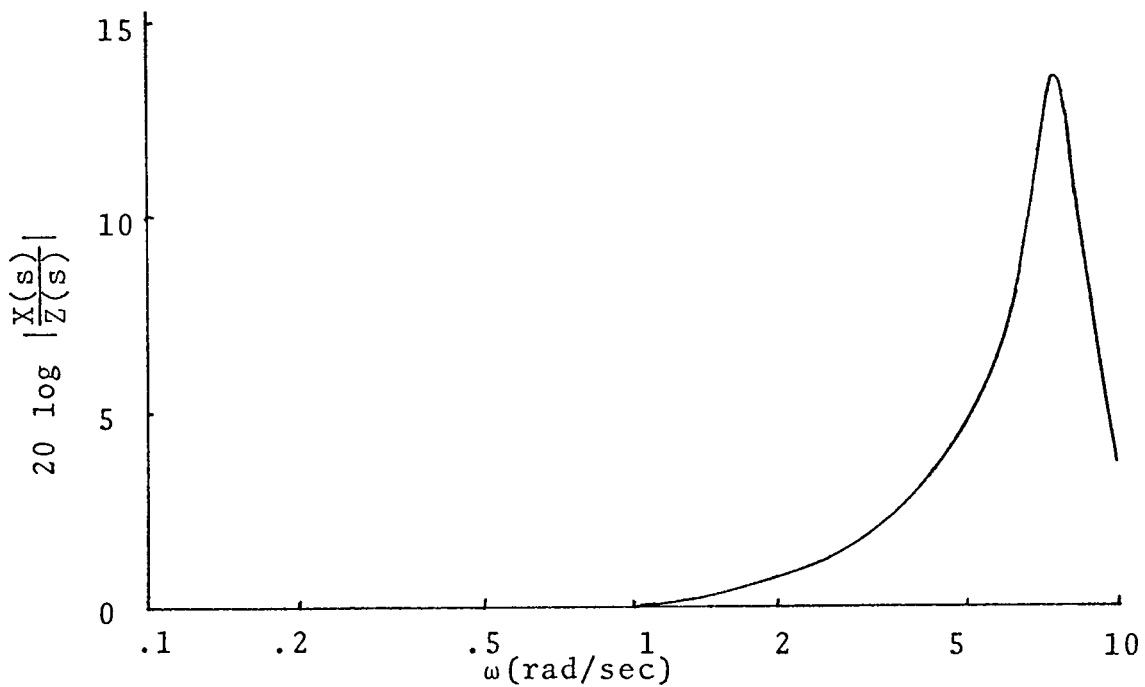


Figure 28. Frequency Response of Drum Motion  
With Respect to Ship Motion  
(Bode Plot)

TABLE 7

FREQUENCY RESPONSE OF PAYLOAD MOTION AND DRUM MOTION  
WITH RESPECT TO SHIP MOTION

$\omega$	$\left  \frac{P(s)}{Z(s)} \right $	$\left  \frac{X(s)}{Z(s)} \right $
.1	.0026	1
.2	.0053	1
.4	.011	.996
.5	.013	.995
.6	.015	.994
.7	.018	.994
.8	.020	.996
.9	.023	.997
1	.025	1.006
1.1	.026	1.013
1.2	.027	1.026
1.3	.028	1.04
1.5	.029	1.07
2	.029	1.17
5.8	.036	4.12
<u>7.6</u>	<u>.073</u>	<u>1.51</u>
10	.023	.59

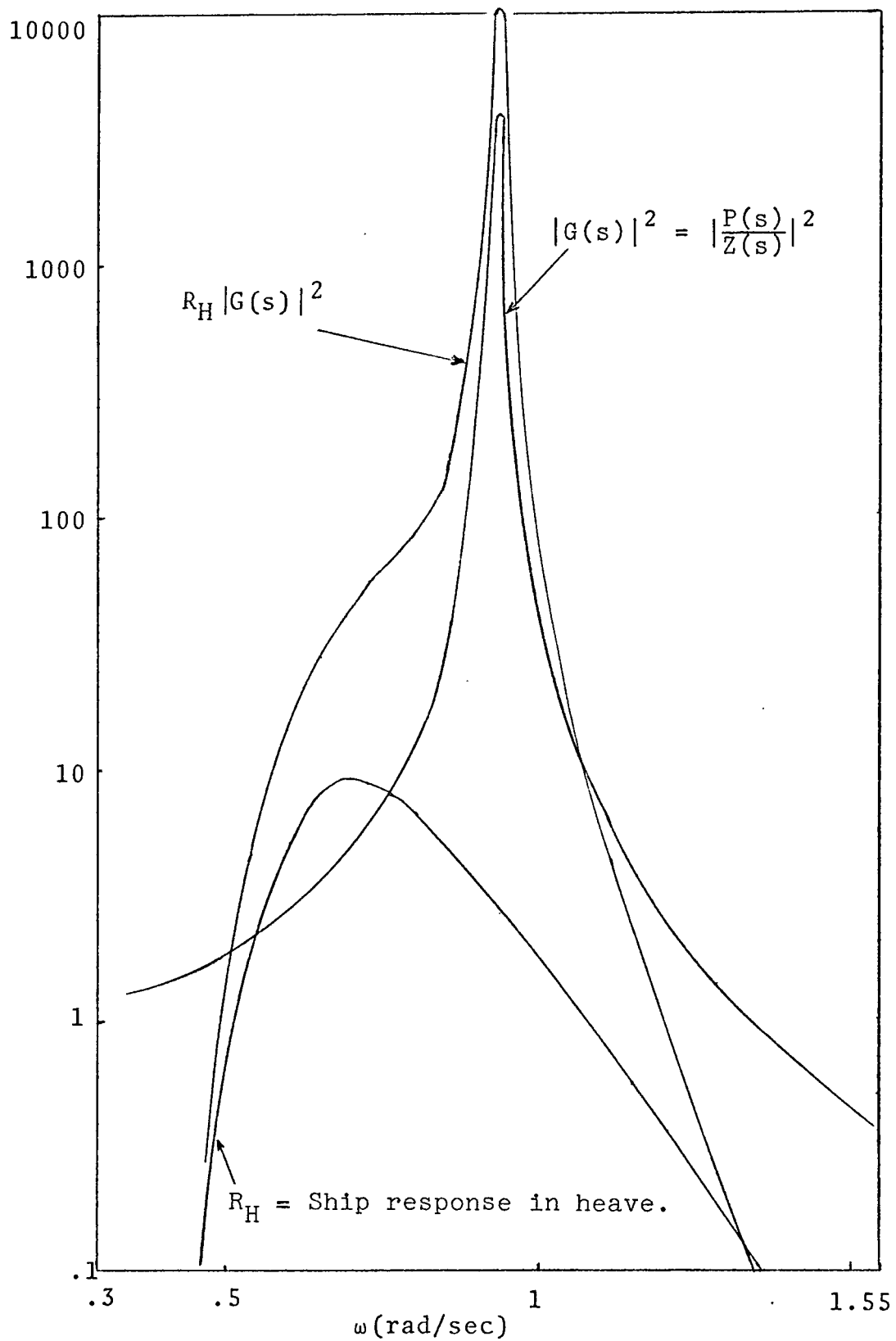


Figure 29. Frequency Spectrum for Payload Due to Heave Motion Before Compensation

TABLE 8

FREQUENCY SPECTRUM FOR PAYLOAD DUE TO HEAVE  
MOTION BEFORE COMPENSATION

$\omega$ (rad/sec)	$ G(s) ^2$ (m/m) <sup>2</sup>	$R_H$ (m <sup>2</sup> -sec)	$R_H  G(s) ^2$ (m <sup>2</sup> -sec)
.34	1.32	0	0
.43	1.58	.0066	.01
.47	1.75	.15	.263
.52	2.04	.9	1.84
.56	2.32	2.75	6.37
.60	2.82	5.05	14.23
.65	3.55	7.92	28.1
.69	4.36	9.05	39.5
.73	6.31	8.68	54.77
.78	9.55	7.37	70.38
.86	31.62	4.71	148.94
.94	3981	2.61	10390
1.03	22.39	1.51	33.8
1.12	6.16	.713	4.4
1.21	2.34	.36	.84
1.29	1.40	.17	.23
1.38	.79	.1	.074
1.46	.54	.06	.03
1.55	.36	.03	.01

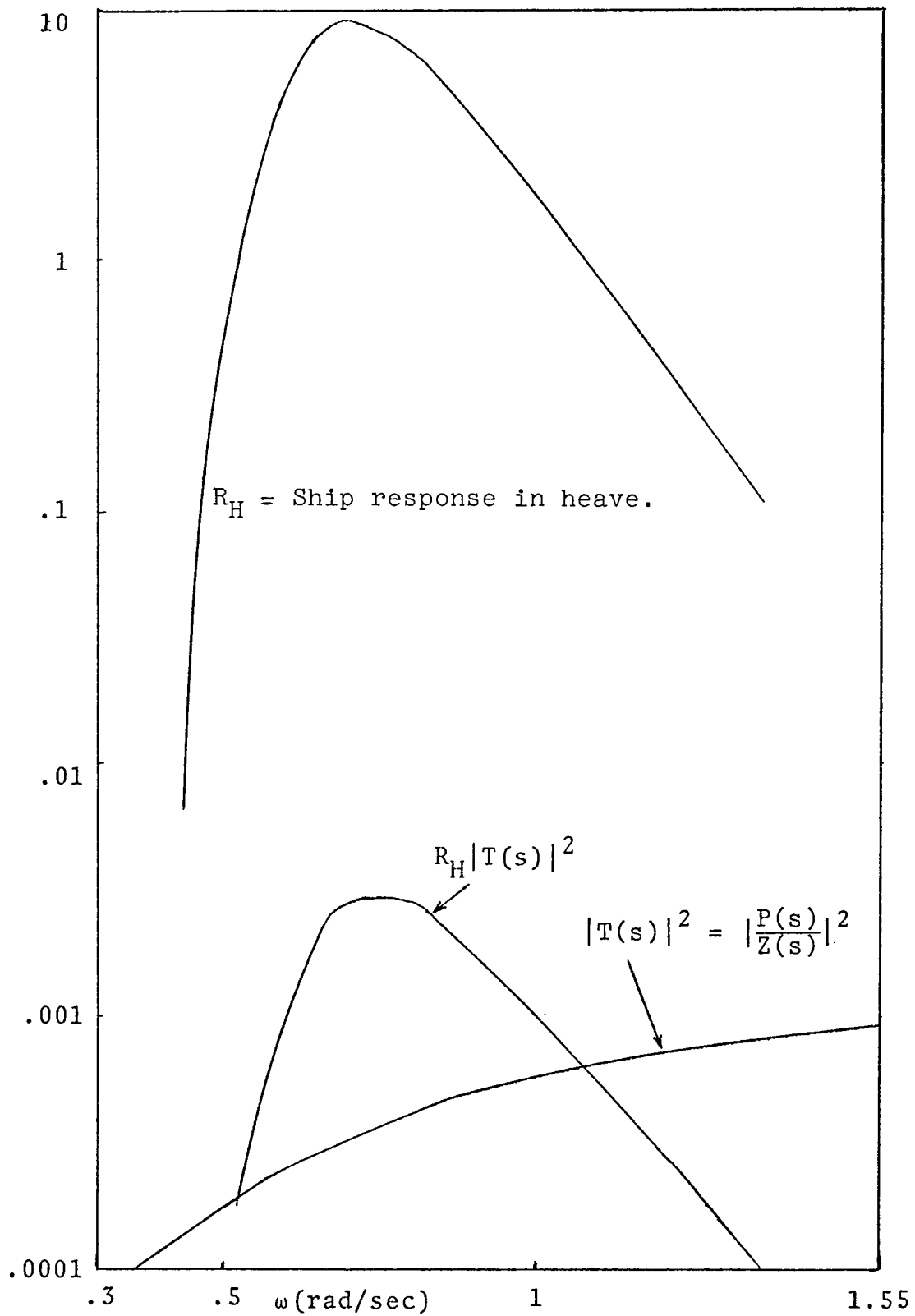


Figure 30. Frequency Spectrum for Payload Due to Heave Motion After Compensation

TABLE 9

FREQUENCY SPECTRUM FOR PAYLOAD MOTION  
AFTER COMPENSATION

$\omega$ (rad/sec)	$10000 \cdot  T(s) ^2$ (m/m) <sup>2</sup>	$R_H$ (m <sup>2</sup> -sec)	$1000 \cdot R_H  T(s) ^2$ (m <sup>2</sup> -sec)
.34	1	0	0
.43	1	.0066	0
.47	1.5	.15	0
.52	2	.9	.18
.56	2.2	2.75	.6
.60	2.4	5.05	1
.65	2.9	7.92	2.3
.69	3	9.05	2.9
.73	3.5	8.68	3
.78	4	7.37	3
.86	5	4.71	2.2
.94	5.5	2.61	1.4
1.03	6	1.51	.95
1.12	7	.713	.5
1.21	7.3	.36	.27
1.29	8	.17	.13
1.38	8.3	.1	.08
1.46	8.6	.06	.05
1.55	9	.03	.03



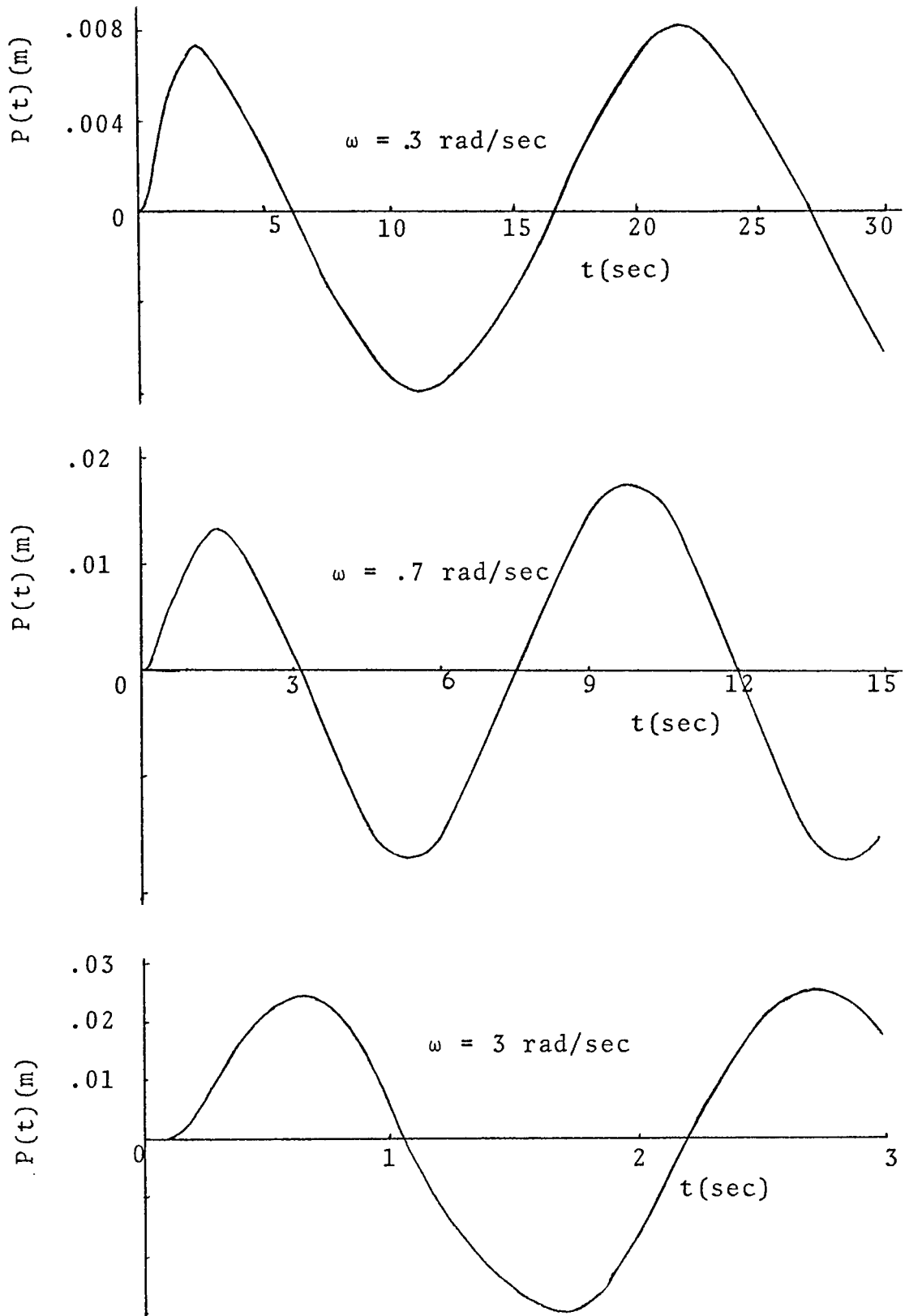


Figure 31. Compensated Payload Motion Due to a Unit Sinusoidal Ship Motion for the Frequencies Shown

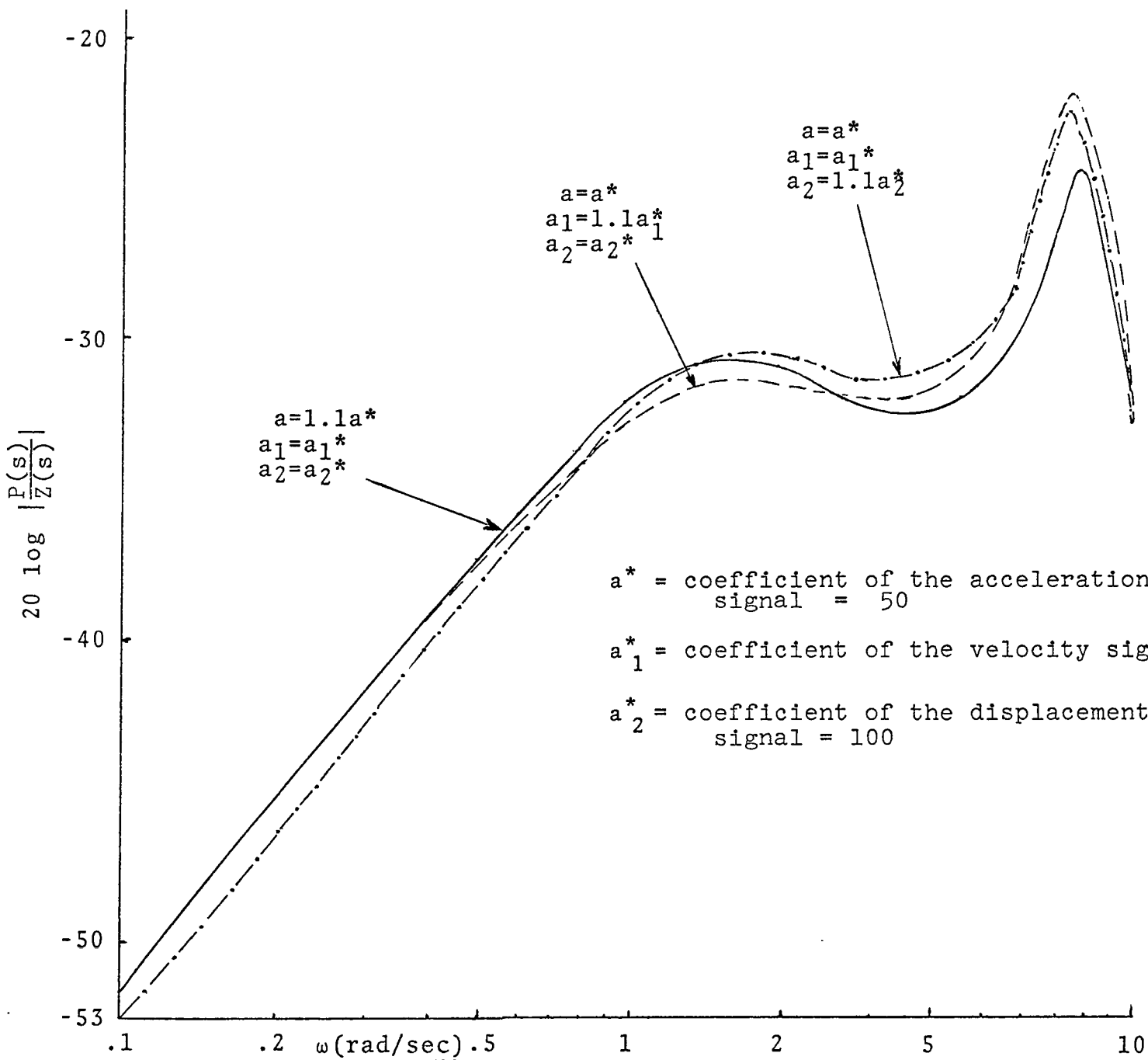


Figure 32. Sensitivity Test

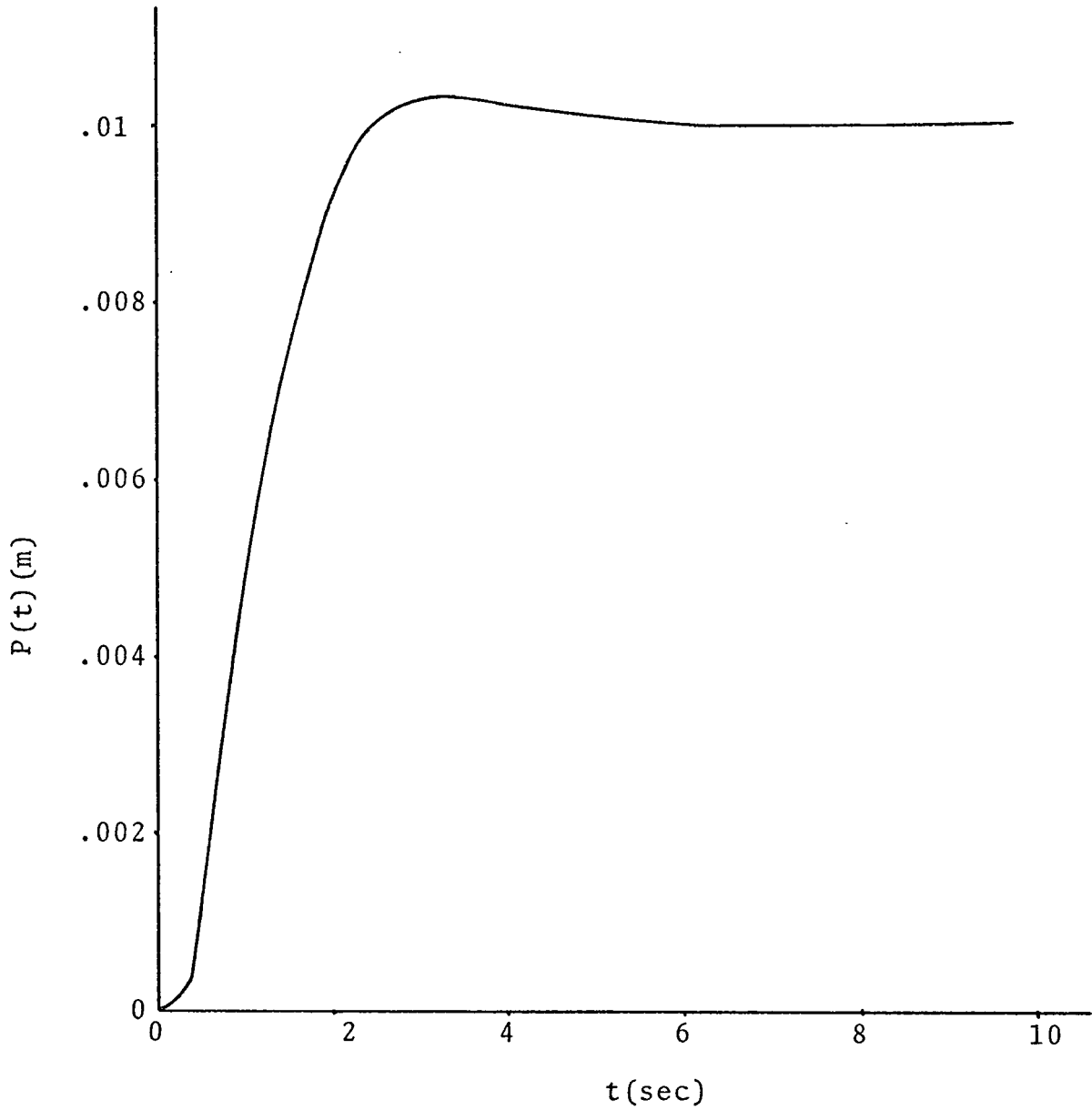


Figure 33. Payload Motion due to a Unit Step  
Voltage Change at Winch Control

Figure 33 shows payload motion due to a unit step voltage ( $E_G(s) = \frac{1}{s}$ ) change at the input to the winch control.

## CHAPTER IX

## CONCLUSIONS

Significant improvement in the reduction of the payload motion due to vessel motion can be obtained by using feedback from the cable end. The most significant improvement is for very low frequency motions such as tidal changes and long period swells. In particular, a payload could be maintained at a relatively fixed position--vertically--with respect to the seafloor for long periods of time.

In addition, the payload motion is immune to disturbing forces applied directly to the payload.

A reduction in the peak cable tension is obtained since the payload motion is limited to very small amplitude; also large transient stress loads due to unexpected violent vessel motions of short duration are virtually eliminated.

Using reasonable assumptions with respect to vessel size, cable lengths and payload masses, a very satisfactory system can be designed which requires a nominal value of winch power.

The most significant problem in the system design is the transmission of the feedback signals. However, several techniques can be used which would provide satisfactory solutions. A hard wire connection between the payload-end

of the cable and the vessel could be utilized; this would add some complexity to the winching system but is not insurmountable and in some circumstances would be well worth the added complexity.

In general, the feedback signal "gains" are not critical for satisfactory system performance. For good low frequency performance, payload displacement information must be one of the feedback signals.

## BIBLIOGRAPHY

1. Weinblum, G. and M. St. Denis, "On the Motions of Ships at Sea," Trans. Soc. Naval Arch. Marine Engrs., Vol. 58, 1950, p. 184.
2. Wiegel, R. L., Oceanographical Engineering, Prentice-Hall, New Jersey, 1964.
3. Roll, H. U., "Height, Length, and Steepness of Seawaves in the North Atlantic and Dimensions of Seawaves as Functions of Wind Forces," Soc. Naval Arch. Marine Engrs. Tech. Res. Bull. 1-19, 1958.
4. Bertschneider, C. L., "Wave Forecasting," Handbook of Ocean and Underwater Engineering, McGraw-Hill, New York, 1969, pp. (11-98)-(11-99).
5. Snyder, A. E., J. C. Jerabek, and C. A. Whitney, "Constant Tension Oceanographic Winch," American Society of Mechanical Engineers, Paper No. 63-WA-335, 1963.
6. Eskinazi, S., Vector Mechanics of Fluids and Magneto-fluids, Academic Press, New York, 1967.
7. Patton, K. T., "Tables of Hydrodynamic Mass Factors for Translational Motion," American Society of Mechanical Engineers, Paper No. 65-WA/UNT-2.
8. Thomson, W. T., Theory of Vibration With Applications, Prentice-Hall, New Jersey, 1972.
9. Fox, R. W. and A. T. McDonald, Introduction to Fluid Mechanics, Wiley, New York, 1973.
10. Hoerner, S. F., The Fluid Dynamics of Drag, 2nd ed. Midland Park, New Jersey, 1965.
11. Gibson, J. E. and F. B. Tuteur, Control System Components, McGraw-Hill, New York, 1958.
12. D'azzo, J. J. and C. H. Houpis, Feedback Control System Analysis and Synthesis, McGraw-Hill, New York, 1966.

13. Churchill, R. V., Operational Mathematics, McGraw-Hill, New York, 1972.
14. Bertschneider, C. L., "Significant Waves and Wave Spectrum," Ocean Industry, Feb. 1968, pp. 40-46.
15. National Academy of Sciences - National Research Council, AMSOC Committee, Division of Earth Sciences, "Design of a Deep Ocean Drilling Ship," National Academy of Sciences - National Research Council, Publication No. 984, Washington, D.C., 1962.



## APPENDIX A [6,7]

## THE CALCULATION OF THE APPARENT OR VIRTUAL MASS

When a body is set in steady motion with respect to the infinite medium at rest, the medium surrounding the body will be set in motion as well. Consequently, the energy required to bring an immersed body to a constant translatory velocity is the sum of the kinetic energy of the body plus the kinetic energy of the fluid particles set in motion. (Energy losses owing to the viscous effects are not taken into account in this discussion).

The apparent mass of a body moving at a velocity  $V$  is then a virtual mass moving at the same velocity. The mass of the fluid particles set in motion is referred to as "added mass," "increased inertia," or "hydrodynamic mass." The sum of this mass and the body's mass is usually designated as the virtual mass.

The force  $F$  to accelerate a body of mass  $m$  is:

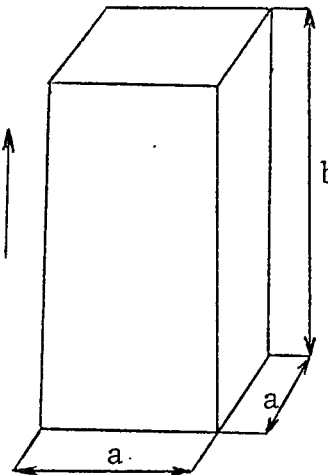
$$F = (m+m_h)a$$

where

$a$  = acceleration

$m_h$  = hydrodynamic mass associated with the particular  
direction of motion

TABLE A-1  
HYDRODYNAMIC MASS FACTOR

Body Shape	Translational Direction	Hydrodynamic Mass																		
	Vertical	$m_h = K \rho a^2 b$ <table><tr><th><math>b/a</math></th><th><math>K</math></th></tr><tr><td>1</td><td>2.32</td></tr><tr><td>2</td><td>.86</td></tr><tr><td>3</td><td>.62</td></tr><tr><td>4</td><td>.47</td></tr><tr><td>5</td><td>.37</td></tr><tr><td>6</td><td>.29</td></tr><tr><td>7</td><td>.22</td></tr><tr><td>10</td><td>.10</td></tr></table>	$b/a$	$K$	1	2.32	2	.86	3	.62	4	.47	5	.37	6	.29	7	.22	10	.10
$b/a$	$K$																			
1	2.32																			
2	.86																			
3	.62																			
4	.47																			
5	.37																			
6	.29																			
7	.22																			
10	.10																			

In Table A-1, the hydrodynamic mass factor for parallelepipeds bodies is shown ( $\rho$  = density of fluid in which the body is immersed).

## APPENDIX B [14]

DETERMINATION OF THE WAVES SPECTRUM FROM SIGNIFICANT  
WAVE HEIGHTS AND WAVE PERIODS

The period spectrum and the frequency spectrum are given by the following equations:

$$S(T) = 3.434 (\bar{H})^2 \frac{T^3}{(T)^4} e^{-.675(T/\bar{T})^4} .$$

The corresponding frequency spectrum is obtained by use of the following manipulation:

$$S(T)dT = -S(f)df$$

$$T = \frac{1}{f}$$

$$dT = -\frac{1}{f^2} df$$

or

$$df = -\frac{1}{T^2} dT$$

With the proper transformation, the frequency spectrum is given by the following:

$$S(f) = 3.434 (\bar{H})^2 \bar{T} (f\bar{T})^{-5} e^{-.675(f\bar{T})^{-4}} .$$

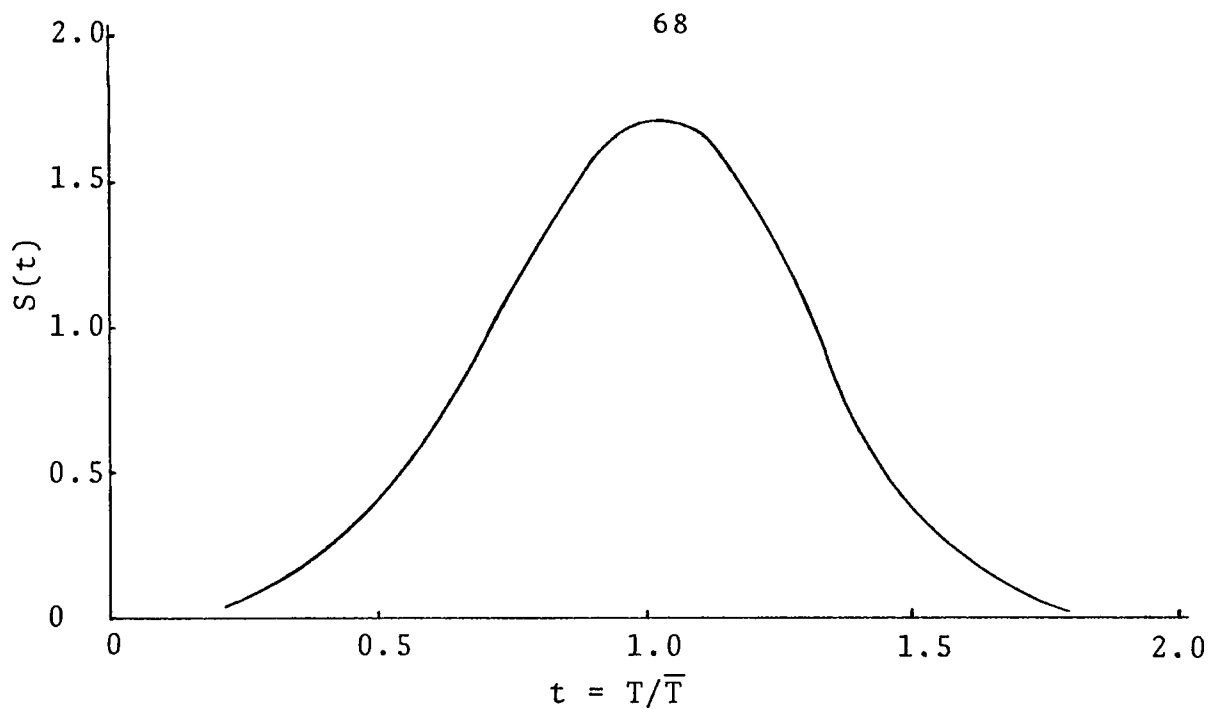


Figure B-1. Non-dimensional Period Spectrum

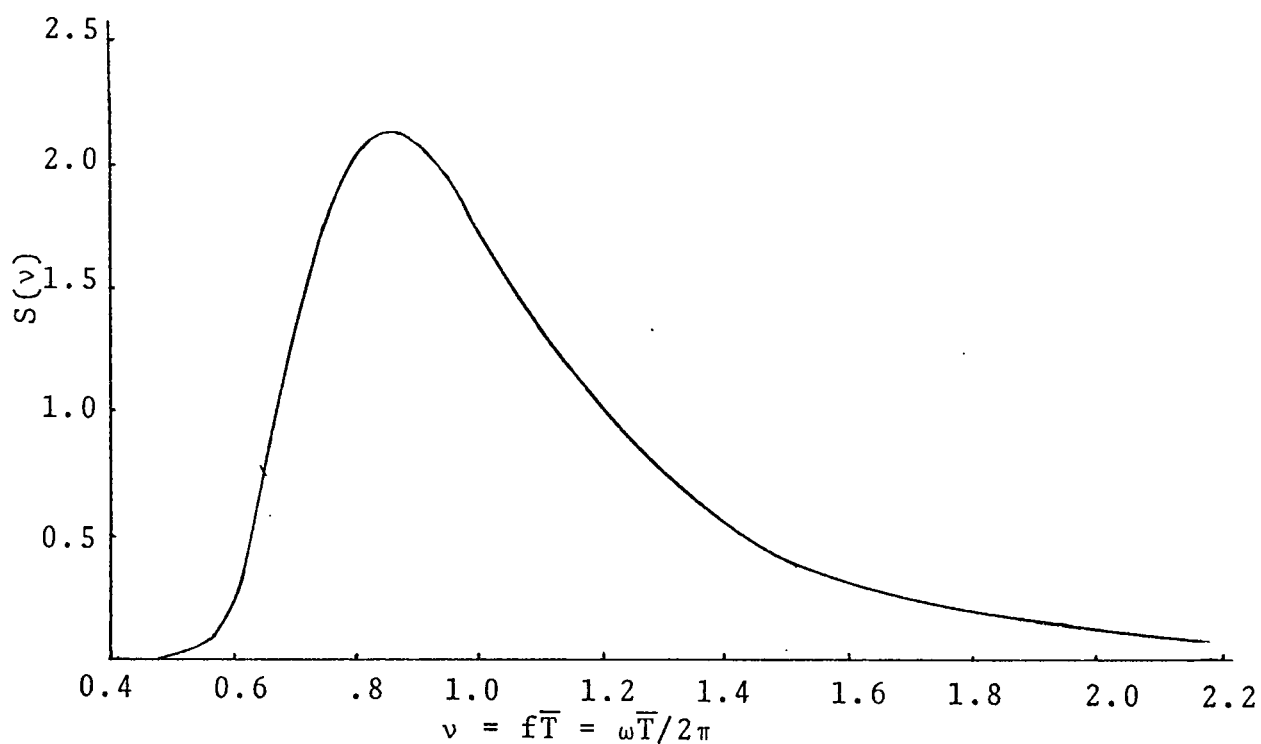


Figure B-2. Non-dimensional Frequency Spectrum

TABLE B-1

## NON-DIMENSIONAL PERIOD SPECTRUM

$t=T/\bar{T}$	$S(t)$
0.1	0.003
0.2	0.025
0.3	0.092
0.4	0.216
0.5	0.412
0.6	0.680
0.7	1.003
0.8	1.335
0.9	1.609
1.0	1.750
1.027	1.754
1.1	1.690
1.2	1.099
1.4	0.707
1.5	0.383
1.6	0.169
1.7	0.061
1.8	0.017
1.9	0.004

$$S(t) = 3.434t^3e^{-0.675t^4}$$

$$S(T) = \frac{(\bar{H})^2}{\bar{T}} S(t)$$

$$T = \bar{T}t$$

$$\overline{H^2} = \int_0^\infty S(T) dT$$

$$\overline{H^2} = \frac{1}{2} H_S^2 = \frac{4}{\pi} (\bar{H})^2$$

TABLE B-2

## NON-DIMENSIONAL FREQUENCY SPECTRUM

$\nu$	$S(\nu)$	$\nu$	$S(\nu)$
0.50	0.0022	1.60	0.296
0.55	0.0465	1.70	0.224
0.60	0.243	1.80	0.171
0.65	0.710	1.90	0.132
0.70	1.24	2.00	0.103
0.75	1.77	2.10	0.0812
0.80	2.02	2.20	0.0636
0.85	2.13	2.30	0.0527
0.90	2.07	2.40	0.0422
1.00	1.75	2.50	0.0346
1.10	1.34	2.60	0.0282
1.20	1.00	2.70	0.0238
1.30	0.735	2.80	0.0198
1.40	0.534	2.90	0.0168
1.50	0.393	3.00	0.0140

$$S(\nu) = 3.434\nu^{-5}e^{-0.675\nu^{-4}}$$

$$S(f) = (\bar{H})^2 \bar{T} S(\nu)$$

$$\overline{H^2} = \int_0^{\infty} S(f) df$$

On the above spectrum equations

$$\bar{H} = .625H_S \text{ m}$$

$$\bar{T} = .9T_S \text{ sec}$$

$$f = 1/\bar{T} \text{ sec}^{-1}$$

The factor .9 in  $\bar{T} = .9T_S$  makes the spectrum in agreement with the international ship structures modification of the Bretschneider spectrum.

Figure B-1 and Table B-1 represent the non-dimensional form of the period spectrum. The actual period spectrum can be obtained according to the instructions given on Table B-1.

The corresponding non-dimensional frequency spectrum is given in Figure B-2 and Table B-2. The instructions for obtaining the true frequency spectrum are given also in Table B-2. The radial frequency is  $\omega = 2\pi f$ . Thus if one multiplies the values of  $f$  by  $2\pi$  and divides  $S(f)$  by  $2\pi$ , then one will obtain  $S(\omega)$  versus  $\omega$ .